ASD-TR-61-203
Part III

THE MECHANICAL PROPERTIES OF TANTALUM WITH SPECIAL REFERENCE TO THE DUCTILE-BRITTLE TRANSITION

TECHNICAL REPORT NO. ASD-TR-61-203, Part III
May 1963

AF Materials Laboratory
Aeronautical Systems Division
Air Force Systems Command
Wright-Patterson Air Force Base, Ohio

Project No. 7351, Task No. 735106

(Prepared under Contract No. AF 33(616)-7173 by the Materials Research Corporation, Orangeburg, New York; G. Abowitz, R. A. Burn, authors.)

NOTICES

When Government drawings, specifications, or other data are used for any purpose other than in connection with a definitely related Government procurement operation, the United States Government thereby incurs no responsibility nor any obligation whatsoever; and the fact that the Government may have formulated, furnished, or in any way supplied the said drawings, specifications, or other data, is not to be regarded by implication or otherwise as in any manner licensing the holder or any other person or corporation, or conveying any rights or permission to manufacture, use, or sell any patented invention that may in any way be related thereto.

Qualified requesters may obtain copies of this report from the Armed Services Technical Information Agency (ASTIA), Arlington Hall Station, Arlington 12, Virginia.

This report has been released to the Office of Technical Services, U.S. Department of Commerce, Washington 25, D.C., for sale to the general public.

Copies of this report should not be returned to the Aeronautical Systems Division unless return is required by security considerations, contractual obligations, or notice on a specific document.

NOTICES

When Government drawings, specifications, or other data are used for any purpose other than in connection with a definitely related Government procurement operation, the United States Government thereby incurs no responsibility nor any obligation whatsoever; and the fact that the Government may have formulated, furnished, or in any way supplied the said drawings, specifications, or other data, is not to be regarded by implication or otherwise as in any manner licensing the holder or any other person or corporation, or conveying any rights or permission to manufacture, use, or sell any patented invention that may in any way be related thereto.

Qualified requesters may obtain copies of this report from the Armed Services Technical Information Agency (ASTIA), Arlington Hall Station, Arlington 12, Virginia.

This report has been released to the Office of Technical Services, U.S. Department of Commerce, Washington 25, D.C., for sale to the general public.

Copies of this report should not be returned to the Aeronautical Systems Division unless return is required by security considerations, contractual obligations, or notice on a specific document.

ABSTRACT

The tensile behavior of single phase tantalum-hydrogen alloys and tantalum-molybdenum alloys containing dilute additions of molybdenum has been studied as a function of grain size and alloying addition. Uniaxial tension tests were carried out at 25°C and -196°C, the strain rate, $\dot{\varepsilon}$, being fixed throughout the experiments at 10^{-3} sec^{-1}. The parameters σ_i and k_y of the Petch equation were evaluated where possible.

It was observed that σ_i, the lattice friction stress, was essentially independent of hydrogen content at room temperature whereas k_y, which was presumably a measure of the solute-dislocation interaction, was observed to increase by the absorption of hydrogen into tantalum. These results are similar to those found by Wilcox for hydrogen in niobium. The increase in k_y is believed to be the result of the hydrogen-dislocation pinning interaction. The insensitivity of σ_i to hydrogen content is postulated to be due to the adsorption of hydrogen not associated with dislocations at the grain boundaries. No evidence of mechanical twinning was found in any of the Ta-H alloys either at 25°C or at -196°C.

The addition of small amounts of Mo to Ta results in an increase in k_y at 25°C which can be attributed to a Mo-dislocation interaction. The rate of increase of k_y per at.% Mo is greater than expected on the basis of a linear variation in k_y between the pure elements. It was also observed that σ_i is unaffected, at 25°C, by the addition of small amounts of Mo. This behavior is not presently understood and raises some doubt as to the physical significance of σ_i. Mechanical twinning was observed in several Ta-Mo alloys at -196°C, but none was observed for these same alloys at 25°C. A large increase in ductility accompanied the twinning.

This documentary report has been reviewed and is approved.

W. J. TRAPP
Chief, Strength and Dynamics Branch
Metals and Ceramics Division
Air Force Materials Laboratory

TABLE OF CONTENTS

LIST OF ILLUSTRATIONS

LIST OF ILLUSTRATIONS
(Continued)

LIST OF TABLES

I. INTRODUCTION:

There have been several treatments of the subject of yielding and the ductile-to-brittle transition in body-centered cubic metals. These are due to Stroh (1)*, Cottrell (2), Petch (3) and quite recently Hahn (4). The theories of Stroh, Cottrell and Petch assume that the binding energy between dislocations and "atmospheres" of interstitial atoms in body-centered cubic metals is the dominant factor in the yield point effect. Hahn has proposed that the locking of dislocations by interstitials is not the dominant factor but rather the yield point behavior can be explained in terms of dislocation multiplication and velocity characteristics in body-centered cubic metals. The importance of these theories of the mechanical behavior of the refractory metals cannot be overestimated, and it would be well to review briefly the various concepts and their implications.

Stroh's viewpoint is that at relatively high temperatures thermal fluctuations will be able to free the dislocations around a pile-up array and so relieve the stresses there. This results in the metal behaving in a ductile manner. At low temperatures where these thermal fluctuations are not large enough to free the dislocations at a significant rate, pile-up arrays will generate sufficient stresses to generate a crack and the metal will be brittle. The probability of brittle fracture is identified by Stroh with the probability that the dislocations in a piled-up array will not be released.

To free a dislocation an activation energy $U(\sigma)$, which is a function of the applied stress, must be supplied. The probability per unit time, ϕ, of the dislocation being freed is

$$\phi = A \exp\left(U(\sigma)/kT\right) \qquad (1)$$

---

*Numbers in parentheses indicate References.

Manuscript released by the authors March 1963 for publication as an ASD Technical Report.

where A is a frequency constant. The mean time elapsing before a dislocation is released, τ, is given by

$$\tau = \frac{1}{A} \exp\left(U(\sigma)/kT\right) \tag{2}$$

The probability that the release of a dislocation will not occur in time t is

$$p = \exp\left(-t/\tau\right) \tag{3}$$

or

$$p = \exp\left[-At \exp\left(-U(\sigma)/kT\right)\right] \tag{4}$$

The variation of p from 0 to 1 as T decreases occurs over a narrow temperature range because of the double exponential term and hence the function typifies a transition effect. The transition will occur at a temperature, T_c, defined as

$$T_c = U(\sigma)/k \ln \phi t \tag{5}$$

This relation is difficult to test experimentally inasmuch as time is not used to describe the transition effect (except indirectly as strain rate) and the stress activation function, $U(\sigma)$ is undefined. This may be a useful correlation between temperature and time at constant stress in delayed failure or static fatigue phenomena.

The correlation between transition temperature, T_c, and the time, t, at the stress level, σ, has been modified by Stroh so that it can be evaluated from experimental data. In the conventional tensile test the time at σ is approximately given as

$$t = \frac{\sigma}{\dot{\sigma}} \tag{6}$$

Actually, the term σ should be that portion of the applied stress which actually generates the dislocation pile-up, $(\sigma - \sigma_0)$.

Since it is more convenient to deal with strain rate $\dot{\epsilon}$ rather than stress rate $\dot{\sigma}$, we can write

$$\dot{\sigma} \approx E \cdot \dot{\epsilon} \tag{7}$$

provided that the total ductile deformation before fracture is small. From the relationship between fracture stress and grain size

$$(\sigma - \sigma_0) = Kd^{-1/2} \tag{8}$$

we can write

$$t = \frac{K}{E\, d^{1/2}\, \dot{\epsilon}} \tag{9}$$

using the relationship $T_c - f(t)$ one obtains

$$\frac{1}{T_c} = -\frac{K}{U} \ln \dot{\epsilon} - \frac{1}{2}\frac{K}{U} \ln d + C \tag{10}$$

where C is a constant independent of T_c, $\dot{\epsilon}$ and d. Thus, with constant grain size material

$$\frac{1}{T} \propto \ln \dot{\epsilon} \tag{11}$$

and with constant strain rate

$$\frac{1}{T_c} \propto \ln d \tag{12}$$

The experimental correlation of Wittman and Stepanov (5) between transition temperature and strain rate for steel agrees with the equation above. Data on the influence of ferrite grain size on

the transition temperature can be found to agree with the above predictions (6). The weakness of the Stroh model is that it does not distinguish between metals which do and do not display the transition phenomenon. This is largely because of the inexplicit nature of the $U(\sigma)$ term.

Cottrell's (2) treatment of the ductile-brittle transition phenomenon differs from Stroh's. It uses a model of two intersecting slip bands from which dislocations coalesce on a cleavage plane as shown in Figure 1. The crack is assumed to form in a plane normal to the applied stress. The energy of the cracked dislocation group is the sum of four terms

$$W = W_1 + W_2 + W_3 + W_4 \tag{13}$$

where

W_1 = energy of the stress field of the dislocation group

W_2 = surface energy of the crack faces

W_3 = elastic energy of the crack in the applied field

W_4 = work done in opening up the crack

Each of these terms is a function of the crack length, C. The equilibrium length of a crack is given by

$$\frac{\partial W}{\partial C} = 0 \tag{14}$$

and the point at which a stable crack becomes self-propatating is defined by

$$\sigma n b = 2 \gamma \tag{15}$$

where n = number of dislocations in the pile-up, b = Burger's

vector, γ = crack surface energy and σ is the applied tensile stress. Eshelby et al., (7) have shown that a piled-up group of n dislocations acted upon by a shear stress, σ_s, will occupy a length of slip line, L, given by

$$L = \frac{G\, bn}{\pi(1-\nu)\,\sigma_s} \tag{16}$$

rearranging, and taking the active shear stress σ_s as

$$\sigma s \simeq \frac{\sigma - \sigma_o}{2} \tag{17}$$

one obtains

$$nb = \frac{\pi(1-\nu)\,(\sigma - \sigma_o)\,L}{2\,G} \tag{18}$$

If we let $L = d/4$ rather than $d/2$, we obtain

$$nb = \frac{\pi(1-\nu)\,(\sigma - \sigma_o)\,d}{8\,G} \tag{19}$$

Since at the transition temperature the crack nucleus forms at or near the yield stress, the term σ should properly be designated as σ_y. Petch (8) has shown that σ_y depends on grain size in the manner

$$\sigma y = \sigma_o + k_y\, d^{-1/2} \tag{20}$$

so

$$\frac{\sigma y\ \pi(1-\nu)\, k_y\, d^{1/2} = 2\,\gamma}{8\,G} \tag{21}$$

or, rearranging

$$\sigma_y \, k_y \, d^{1/2} = \beta G \gamma \tag{22}$$

with $\nu \approx .3$ and $l = d/4$, $\beta \approx 7$

The significance of this relationship is that if the right hand side is larger than the left ductile behavior can be expected, whereas if the left hand side is larger, brittle behavior will result. The intrinsic yield stress σ_y is the dominant term since it can be varied widely by temperature, strain rate and structure.

Petch (3) has developed essentially the same relationship governing the ductile-brittle transition. The transition from ductile to cleavage fracture is deemed to signify the ability of a slip band nucleated crack to propagate as a Griffith-Orowan crack. Thus, the stress to nucleate a crack is more than sufficient to propagate it.

From Stroh (1) the condition for crack nucleation is taken as

$$nb \, \sigma (1 + 1/\sqrt{2}) = 4 \gamma \tag{23}$$

where γ here is the surface energy corrected for the plastic work as in the Griffith-Orowan relationships. As before

$$n = \frac{\pi (1 - \nu) (\sigma - \sigma_o) \, d}{4 G b} \tag{24}$$

where Petch uses $L = d/2$ rather than the $L = d/4$ favored by Stroh. Equating these two equations one obtains

$$\sigma (\sigma - \sigma_o) \, d \simeq 4 G \gamma \tag{25}$$

Using the grain size relationship to fracture

$$(\sigma - \sigma_o) = k\, d^{-1/2} \tag{8}$$

the condition for crack nucleation is

$$\sigma\, k\, d^{1/2} \simeq 4\, G\, \gamma \tag{26}$$

At the transition $\sigma \simeq \sigma_y$ and $k = k_y$, so

$$\sigma_y\, k_y\, d^{1/2} \simeq 4\, G\, \gamma \tag{27}$$

which is identical in form with the Cottrell condition for transition and differs by the numerical coefficient on the right hand side.

The criterion developed by Cottrell and Petch describes the interplay of parameters at the transition but does not predict the transition temperature itself. Petch (9) has recently derived the following expression for the transition temperature

$$\beta\, T_c = \ln B - \ln \left[\frac{4_q\, G - k}{k}\right] - \ln d^{-1/2} \tag{28}$$

where

$$\sigma F = \sigma_o + k\, d^{-1/2} \tag{29}$$

and $\ln \sigma = \ln B - \beta T$, q is a stress concentration factor and k, β, B are characteristic parameters of the material. The temperature, strain rate and compositional dependence of the resolved shear stress are bound up in the σ_o term which represents the aggregate of terms resisting the movement of dislocations on a slip plane.

The use of σ_o in the transition analysis is more fundamental to the dislocation movement processes and is therefore more meaningful than the use of the engineering yield stress, σ_y. This also serves to emphasize that fracture and yield are inseparable in nature but that exceeding the engineering yield stress is not a necessary prerequisite of fracture. The Petch relationship provides for a grain size dependence of the

transition temperature of the form

$$T_c \propto \ln d \tag{30}$$

This is not compatible over a large range of grain sizes with the Stroh relationship

$$\frac{1}{T_c} \propto \ln d \tag{12}$$

The present body of evidence (9) favors the Petch equation.

The general tendency for body-centered cubic metals to show a transition behavior can be correlated by the Cottrell-Petch criterion with the sharp rate of increase in yield strength at low temperatures. This is characteristic of the elements Fe, Cr, V, Mo, Nb, Ta and W. In all cases, the yield strength rises by a factor of three or more over the temperature range in which ductility is dropping sharply. In contrast, the yield strength of copper is much less dependent on temperature and the $\sigma_y k_y d^{1/2}$ term is small at all temperatures resulting in ductile behavior. It is possible to observe brittle behavior in metals such as copper, if the γ term on the right hand side is varied. The γ term can be varied widely be contacting the specimen with various different liquid metals. In this manner, i.e., liquid metal embrittlement, face-centered cubic metals can be made to show a transition from ductile-to-brittle behavior.

Hahn (4) has suggested a model to account for the phenomena of yielding, the Lüders' band and the delay-time in body-centered cubic metals based on the work of Gilman and Johnston (10, 11, 12) in LiF. Hahn cites many pieces of evidence which indicate that the concept of the tearing dislocations away from their pinning points as the dominate factor in such yield effects as the abrupt yield drop (13), Lüders' strain and Lüders' band propagation (14) and the delay-time phenomenon (15) is not satisfactory. The alternate approach involves the heterogeneous nucleation of new dislocations, the rapid multiplication of the dislocations and the stress dependence of the dislocation velocity.

Utilizing this approach Hahn has been able to quantitatively account for many features of the yielding behavior of body-centered cubic metals and to overcome some of the difficulties

encountered by the unlocking approach of Cottrell and Petch. Some of these difficulties were the presence of sharp yield points in single crystals, $d^{-1/2}$ dependence of the flow stress in face-centered metals which undergo no discontinuous yielding and the similar temperature, strain rate and grain size dependence of the upper and lower yield stress and flow stress values. It is difficult to apply the dislocation locking concept to both the yield and flow stress dependence. The concept of dislocation unlocking is not excluded by the "dislocation dynamics" approach, but it is relegated to a minor role in the yielding behavior. Unfortunately, the theory does not treat the grain size dependence of the yield stress.

During the past two years, the influence of interstitial impurities on the mechanical properties of tantalum has been extensively studied at Materials Research Corporation (16, 17). The influence of carbon and oxygen upon the parameters in the Petch equation have been evaluated. Oxygen has been shown to be more effective than carbon in restricting dislocation motion. The presence of a second phase, TaC, was found to have a more pronounced effect on the rate of work hardening than on the magnitude of the flow stress. It is the purpose of the present work to study the effect of the interstitial element hydrogen upon the mechanical properties of tantalum and also the mechanical behavior of Ta-Mo alloys in which the Mo atom assumes a substitutional position in the lattice. The tensile properties will be examined as a function of both composition and temperature, and the results interpreted in terms of the fundamental theories discussed previously.

II. EXPERIMENTAL PROCEDURE:

A. Tantalum-Hydrogen Alloys

Sintered tantalum rods 15" long by 1/4" in diameter of 99.9% purity were obtained from the Kawecki Chemical Company. These rods were given two to three passes in the MRC floating zone electron beam refiner. The chemical analysis* of "as-received" material is given in Table I.

The electron beam refined tantalum was then subjected to various working and annealing schedules to attain the desired grain sizes. Reductions in area in the range of 25 to 75% were accomplished at room temperature by various combinations of

---

*All anaylses on refined material reported in this study were performed by the National Research Corporation.

rolling, swaging, and hammer forging. Subsequent recrystallization annealing heat treatments were performed either by electron beam heating in vacuum or by self-resistance heating under a positive pressure of argon or helium. Recrystallization temperatures in the electron beam method ranged from 1000°C to 1800°C. The hot zone traversed the length of rod at a rate of 0.25" per minute. Self-resistance heating quickly recrystallized an entire rod within 5 to 30 seconds at temperatures between 1400°C and 2200°C.

The recrystallized tantalum rods were cut into 2" specimen lengths. The ends of the specimens were carefully threaded to facilitate gripping the specimens in the tensile tests. A central reduced section gage length was chemically machined in each specimen utilizing an etch consisting of one part HNO_3 and one part HF.

The tensile specimens were prestrained one-quarter per cent in tension to assure proper alignment and were given a recovery anneal at 800°C for 1 hour in a vacuum of 5×10^{-5} Torr. The specimens were carefully wrapped in tantalum foil which served as a getter. Subsequent to the recovery anneal the specimens were charged with hydrogen.

Charging involved adsorption of gaseous hydrogen from the vapor phase utilizing a Sieverts' type apparatus. This method enables one to control both the temperature and partial pressure of hydrogen surrounding the specimens. The apparatus is shown schematically in Figure 2. It was found that a high temperature vacuum annealing treatment was necessary immediately prior to hydrogen charging to remove surface oxides that would otherwise impede adsorption and result in little hydrogen pickup. The vacuum anneal was carried out in a dynamic vacuum of 5×10^{-5} Torr at 900°C for 1 hour. Without removing the specimens from the vacuum chamber the temperature was then lowered to between 500°C and 600°C, depending upon the amount of hydrogen to be absorbed The vacuum chamber was then isolated from the pumping system and hydrogen was admitted into the system until a partial pressure of approximately 700 mm Hg. was reached. Temperature and hydrogen pressure were maintained for 1 and 2 hours. A rapid rate of cooling the specimens was achieved by removing the furnace from the specimen area.

The hydrogen charged specimens were then threaded into tensile grips and further cemented into the grips with an epoxy resin. Tensile tests were carried out at both 300°K and 77°K.

B. Tantalum-Molybdenum Alloys

To prepare the Ta-Mo alloys, small rods or wires of molybdenum were inserted in a longitudinal groove previously machined into an "as-received" 1/4" diameter tantalum rod. The assembly was then swaged together to a rod diameter of 3/16". Each rod was then electron beam melted three times to achieve homogeneity in the alloy. All of the alloy rods were subjected to the same fabrication schedule. They were rolled and swaged to 0.090" diameter at room temperature and then given a recrystallization anneal in the electron beam or in the self-resistance heating apparatus.

Tensile test specimens were made by welding the ends of 2" lengths of the recrystallized alloy to threaded steel collars. Welding at the junction of each collar and specimen was carried out in the electron beam unit under vacuum. Good alignment was insured by drilling central holes, which were close to the size of the specimen diameter, in the threaded collars. The electron beam welding operation produced neat, regular fillets and left an unaffected 1" gage length.

C. Tensile Tests

Tensile tests were carried out at 300°K and 77°K in a "hard" machine of the same basic design as that previously described by Adams (18). A strain rate of 10^{-3} sec^{-1} was used throughout the course of the present work. Load extension curves were autographically recorded on a millivolt recorder whose response time, 1/4 second for full scale deflection, allowed the use of maximum sensitivity (10" full scale) under all testing conditions. The specimens were approximately 0.090" diameter over a 1" gage length. Subsequent to tensile testing the specimens were cut into several sections and both transverse and longitudinal sections were examined metallographically. The material not used for metallographic observations was utilized for chemical analysis.

Grain size measurements were made by metallographic examination of each individual specimen after fracture. The average grain diameter was determined by counting the number of grains intersecting a diameter marker. The cross section was taken in the gage section, outside the necked region, and corrections were applied for grain size reduction as a result of the uniform reduction in area. It was generally observed that the grains were equiaxed with the ratio of the transverse to longitudinal grain diameters being close to unity. In most extreme cases, the ratio of longitudinal to transverse grain diameter was approximately two and in these instances, the grain diameter reported is the average of the transverse and longitudinal diameters. The quantity 2d was used as the measured grain diameter. Therefore, the quantity d, used in all subsequent calculations of k_y, refers to 1/2 the measured grain diameter.

III. EXPERIMENTAL RESULTS:

A. Tantalum-Hydrogen Alloys

Six groups of tensile specimens were successfully charged with hydrogen and these are designated according to "charge number". The hydrogen contents, as analyzed by NRC are reported in Table IV. It should be noted that these contents are all within the room temperature solubility limit as given in reference (19). Metallographic examination of all alloys verified the fact that the hydrogen charged specimens are indeed single phase alloys with no evidence of hybride formation. Table IV also shows, in addition to the hydrogen content, the carbon, oxygen and nitrogen contents of the alloys. Data for beam refined tantalum is included for comparison purposes*. The total interstitial content varies from 70 ppm for pure tantalum to approximately 500 ppm for the most heavily charged specimen.

Figure 3 shows representative tensile curves for the various Ta-H alloys tested at room temperature and at a strain rate of 10^{-3} sec^{-1}. Figure 4 illustrates the tensile behavior of these alloys at liquid nitrogen temperature (-196°C) and the same strain rate of 10^{-3} $sec.^{-1}$. The actual tensile test data for each specimen of each charge are given in Table II. Grain size in $d^{-1/2}$, lower yield stress, upper yield stress, maximum tensile stress and elongation are tabulated.

Figure 5 shows the lower yield stress versus $d^{-1/2}$ for the six charges at 25°C. Figure 6 illustrates the maximum tensile stress plotted against $d^{-1/2}$ for the same alloys at 25°C. In both Figures 5 and 6 a linear relationship exists between the stress and $d^{-1/2}$ for high purity Ta is shown clearly in Figure 7 which is taken from reference (17). Table VI lists the intercept (σ_i) and slope (k_y) values in c.g.s. units.

In Figure 8 the maximum tensile stress has been plotted as a function of both hydrogen content and total interstitial content. The data for each alloy has been chosen at two points, one being for a $d^{-1/2}$ value of four ($mm^{-1/2}$) and the other for a $d^{-1/2}$ value of zero, i.e., the M.T.S. versus $d^{-1/2}$ curve has been extrapolated to the ordinate. The data are given in Table V. Notice that for each value of $d^{-1/2}$ the curves are similar whether one plots hydrogen content or total interstitial content, the only difference being a displacement of the curves along the abscissa.

---

* The beam refined tantalum containing 70 ppm interstitials is henceforth referred to as pure tantalum in the text.

B. Tantalum-Molybdenum Alloys

Table III shows the measured tensile parameters for all the Ta-Mo alloys. Measurements were made at both 25°C and -196°C at a strain rate of 10^{-3} sec^{-1}. Figure 9 illustrates typical tensile curves for the 0.47 and 0.87 at.% Mo alloys at room temperature. Figure 10 illustrates the -196°C tensile behavior for these same two alloys in cases where no low temperature twinning was observed. In some specimens of the higher Mo contents, i.e., 0.87 and 1.60 at.% Mo, extensive twinning was observed at liquid nitrogen temperatures and this was accompanied by a much greater low temperature ductility than is observed in the absence of twinning. Figure 11 shows the tensile behavior typical of specimens which underwent twinning. Notice the ductility. Metallographic examination showed the presence of twins as shown by Figure 12. The analyzed Mo content of the Ta-Mo alloys is given in Table IV.

Lower yield stress versus $d^{-1/2}$ at 25°C for all the Ta-Mo alloys is shown in Figure 13. The values for pure Ta are included for comparison. Unfortunately, these alloys do not exhibit a well-defined lower yield point at -196°C and, hence these low temperature plots are unavailable. Figure 14 illustrates the dependence of the upper yield stress on $d^{-1/2}$ for pure Ta and the Ta-Mo alloys at room temperature and at -196°C for the 0.87 and 1.60 at.% Mo alloys. A similar correlation of stress versus $d^{-1/2}$ is obtained if one plots the maximum tensile stress against $d^{-1/2}$. This can be seen in Figure 15. If one plots the total elongation as a function of grain size, a large amount of scatter is observed as shown in Figure 16 and no significant correlation is readily seen. Table VII lists the values of the slope, k_y, and the ordinate intercept σ_i, obtained from Figure 13 for the 0.87 and 1.60 at.% Mo alloys. The values of σ_i and k_y for pure Ta under the same test conditions are also included for comparison. Figure 17 shows the k_y values determined from the present study as a function of Mo content. For comparison purposes the line expected, based on a linear compositional variation of k_y between pure Mo and pure Ta, is also shown in Figure 17.

IV. DISCUSSION:

A. Tantalum-Hydrogen Alloys

A plot of lower yield stress versus $d^{-1/2}$ for all the Ta-H alloys, at a fixed temperature of 25°C and a fixed strain rate

of 10^{-3} sec^{-1}, exhibits a linear relationship of the Petch type as shown in Figure 5. The resultant values of σ_i and k_y are given in Table VI. Although considerable experimental scatter exists it is observed that σ_i is essentially independent of hydrogen content. There is apparently no better correlation of σ_i with either oxygen or total interstitial content. Gilbert et al., (21) found no differences in σ_i, within experimental error, for tantalum in which the predominent interstitial impurity was either oxygen, carbon or nitrogen. The results of Murray and Burn (17) on tantalum containing approximately 120 ppm carbon also indicated very little change in σ_i from the value for high purity tantalum even though most of the carbon was in the form of fine carbide particles. The present results indicate that the insensitivity of σ_i to the oxygen, nitrogen and carbon content can be extended to include hydrogen insofar as the temperature and strain rate of the present investigation is concerned. It should be noted that the present results for hydrogen in tantalum are similar to those of Wilcox (22) for hydrogen in niobium which also indicate that σ_i is relatively insensitive to hydrogen content.

The variation of k_y with hydrogen or total interstitial content again shows considerable scatter but it appears that there is a definite increase in k_y with increasing hydrogen content. Again this result is similar to that found by Wilcox (22) for hydrogen in niobium. k_y, which is a measure of the locking strength, i.e., the solute-dislocation interaction energy, is increased when hydrogen is adsorbed in either tantalum or niobium. Oxygen and nitrogen in tantalum have been shown to produce a similar effect on k_y (21). On the other hand carbon in tantalum has been shown to lower the k_y value by a factor of approximately 2.5 as compared with the pure tantalum value (17). This has been attributed to the presence of a second phase carbide particles and their subsequent behavior as sources of mobile dislocations.

In terms of the Petch analysis, hydrogen in solution in tantalum does not affect σ_i, the lattice friction stress, but does raise k_y which is a measure of the pinning strength. In this respect hydrogen behaves no differently than oxygen or nitrogen in tantalum. The reason why σ_i is unaffected is thought to be the fact that the hydrogen in the lattice is associated with dislocations in the form of "atmospheres" and the remainder has diffused to grain boundaries. In this case the bulk lattice remains relatively unperturbed by the addition of hydrogen. k_y increased as a result of the increased interaction between hydrogen and the dislocations. The fraction of the interaction energy that is elastic and that which is electrical in nature is not presently

known. There is reason to believe, based on the large increase in yield and flow stress of molybdenum containing hydrogen (23), that there is a strong electrical interaction between hydrogen and dislocations.

The maximum tensile stress versus $d^{-1/2}$ is shown in Figure 6 for the Ta-H alloys. Once again a linear variation of the Petch type is observed. The intercept on the ordinate correlates fairly well with the hydrogen content of the alloy. The significance of why this "equivalent σ_i" correlates with hydrogen content and not the true σ_i is not understood. This effect, i.e., the grain size dependence of the upper and lower yield stress and the subsequent flow stress being similar, has been observed previously (20) and lends support to the criticisms of the Petch analysis. The argument raised is that at ambient and lower temperatures the flow stress cannot be governed by an unlocking mechanism since at these strains the dislocations are unlocked and the temperature precludes the solutes migrating with the dislocations.

It can be seen from Figure 6 that the maximum tensile stress is raised by the addition of hydrogen for all grain sizes and roughly in proportion to the amount of absorbed hydrogen. As pointed out above, it is reasonable to assume that the moving dislocations are free of their interstitial atmospheres at the stated test conditions. Furthermore, if the bulk of the grain volume is free of dissolved interstitial atoms, as is indicated by the approximately constant σ_i values, then the only remaining means by which the flow stress, in this case the maximum tensile stress, can be increased with increasing interstitial content is by the grain boundaries having a high strength due to adsorbed interstitial atoms. The resistance of the grain boundary to plastic deformation can be expected to vary in proportion to the surface concentration of adsorbed interstitial solute. The increase in maximum tensile stress or flow stress with decreasing grain size stems from the small stress concentrations developed by dislocation pile-ups during deformation of the smaller grains coupled with the increased grain boundary strength due to adsorbed solute. This effect overrides the consideration of a lower adsorbed grain boundary concentration with decreasing grain size for a fixed amount of solute.

Careful metallographic examination was made for the presence of mechanical twins in all of the alloys tested, both at 25°C and -196°C. No evidence of twinning was found. No twin discontinuities or audible clicks were observed during the tensile tests.

The mode of fracture for all alloys at both 25°C and -196°C was fibrous and ductile. Necking in the specimens at 25°C continued to a point whereas at -196°C it was much less extensive.

B. Tantalum-Molybdenum Alloys

Figure 13 shows the lower yield stress plotted against $d^{-1/2}$ for pure tantalum and the Ta-Mo alloys. The experimental scatter in the yield stress data is such that it is difficult to separate the data of the two most dilute alloys, 0.47 and 0.69 at.% Mo, from that of pure tantalum at 25°C and $\dot{\epsilon} = 10^{-3}$ sec^{-1}. As a result, no significant change in σ_i or k_y can be detected, within experimental error, for concentrations of Mo of 0.47 and 0.69 at.%.

For the alloys containing 0.87 and 1.60 at.% Mo a clear effect is shown at these test conditions. The lattice friction stress σ_i, is unchanged from that of pure tantalum and the interaction parameter k_y is increased significantly and in proportion to the Mo content. Figure 17 illustrates the dependence of k_y on Mo content at the test conditions of 25°C and $\dot{\epsilon} = 10^{-3}$ sec^{-1}. Notice that k_y increases much more rapidly with Mo content than would be expected if a linear variation of k_y existed between pure Ta and pure Mo. The linear variation is indicated by the dashed line in Figure 17. The actual values of σ_i and k_y are given in Table VII. It is difficult to interpret this result in terms of the Petch analysis since the lattice friction stress, σ_i, or at least the structurally dependent part of this term, i.e., the non-thermally activated component would be expected to increase markedly due to the large concentration of substitutional Mo atoms present in the lattice. The increased k_y value implies that an interaction exists between the substitutionally dissolved Mo atoms and the dislocations. However, there is more than enough solute present to saturate all the dislocations and the question arises as to the distribution and effect of the remaining solute. Regardless of how the remaining solute may be distributed, homogeneously or heterogeneously, it is difficult to account for the value of σ_i remaining unchanged from that of pure Ta. At 77°K no well-defined yield points were observed and hence a similar analysis could not be made.

The results of Tedmon and Ferriss (24) on the dependence of yield stress on grain size for a 10% tungsten - 90% tantalum alloy also show a behavior at variance with the usual interpretation of the Petch analysis. They observed k_y to be essentially zero indicating that the dislocations were not locked by impurity atoms. Yet, the interstitial content of the alloys was more than sufficient to lock the dislocations. On the other hand, a large

increase in σ_i was observed for their Ta-W alloy as compared to pure tantalum.

The present evidence in Ta-Mo alloys of no change in σ_i and and increase in k_y together with the data for Ta-10% W of an increase in σ_i together with no change in k_y are inexplicable in terms of the Petch analysis and raise the question of the true significance of the σ_i and k_y terms.

Figure 14 illustrates the dependence of the upper yield stress on grain size. At 25°C, the ordinate intercept "σ_i" is again found to remain unchanged for the pure tantalum value while "k_y" again increased. At -196°C, "σ_i" is observed to increase markedly and "k_y" also increases somewhat over that for pure tantalum. To carry the comparison still further, the maximum tensile stress is plotted against $d^{-1/2}$ in Figure 15. At 25°C it is clear that both "σ_i" and "k_y" increase with the addition of molybdenum to tantalum. Also, at -196°C "σ_i" and "k_y" increase with increasing molybdenum content. In this respect, the application of the equation $\sigma = \sigma_i + k_y d^{-1/2}$ at some value of strain, ϵ, where σ is now σ_{flow} rather than σ_{lyp} seems to fit the experimental data. Of course, the original interpretation of σ_i and k_y are no longer valid at these large values of strain and a new interpretation should be sought.

The elongation to fracture versus grain size is shown in Figure 16. There is considerable experimental scatter and there appears to be no clearly discernable trend. Evidence of mechanical twinning was observed during the tensile tests in several 2.3 at.% Mo alloys at -196°C. Two tensile curves illustrating the formation of twins during the tensile test are shown in Figure 11. Careful metallographic examination of the tensile specimens gave visual evidence of the twinning as seen in Figure 12. It should be noted that the occurrence of twinning during deformation at -196°C resulted in a large amount of ductility, roughly five times the ductility of pure tantalum under these same test conditions. Figure 12 also shows representative microphotographs of large and small grain sizes, and typical fracture patterns at both 25°C and -196°C. At both temperatures ductile fibrous type fractures were observed.

V. CONCLUSIONS:

(1) σ_i is independent of the hydrogen content of otherwise pure tantalum at room temperature and at a strain rate of 10^{-3} sec^{-1}.

(2) k_y is increased by the absorption of hydrogen into tantalum.

(3) There is a linear variation between the maximum tensile stress and $d^{-1/2}$ for Ta-H alloys.

(4) Mechanical twinning does not occur in Ta-H single phase alloys at either 25°C or -196°C at a strain rate of 10^{-3} sec^{-1}.

(5) Several at.% Mo in Ta results in an increased k_y but an unchanged σ_i at 25°C. The fact that σ_i does not increase with the large amount of substitutional solute raises the question as to the correctness of the original interpretation of σ_i as a lattice friction stress.

(6) Mechanical twinning was observed in several Ta-Mo alloys at -196°C and $\dot{\epsilon} = 10^{-3}$ sec^{-1}. A large amount of ductility is introduced at -196°C by the occurrence of twinning. These alloys did not twin at 25°C.

(7) At T = 25°C and $\dot{\epsilon} = 10^{-3}$ sec^{-1}, there is no correlation of the total elongation with grain size for all the Ta-Mo alloys tested.

(8) The rate of increase of k_y (T= 25°C, $\dot{\epsilon} = 10^{-3}$ sec^{-1}) with added Mo is much greater than that expected on the basis of a linear variation of k_y between the pure Ta and pure Mo values.

VI. REFERENCES

1. Stroh, A.N., Advances in Physics, 6, 418 (1957).

2. Cottrell, A.H., Trans. AIME, 212, 192 (1958).

3. Petch, N.J., Phil. Mag., 1, 331 (1956).

4. Hahn, G.T., Acta Met., 10, 727 (1962).

5. Wittman, F., and Stepanov, W., J. Tech. Phys. (USSR), 9, 1070 (1939).

6. Hodge, J.M., Manning, R.D., and Reichhold, H.M., Trans. AIME, 185, 233 (1949).

7. Eshelby, J.D., Frank, F.C., and Nabarro, F.R.N., Phil. Mag., 42, 351 (1951).

8. Petch, N.J., J. Br. Iron Steel Inst., 174, 25 (1953).

9. Petch, N.J., "Fracture" Proc. Swampscott Conf., J. Wiley & Sons (1959).

10. Gilman, J.J., and Johnston, W.G., "Dislocations and Mechanical Properties of Crystals", J. Wiley & Sons, p. 116 (1957).

11. Gilman, J.J., J. Appl. Phys., 30, 1584 (1959).

12. Johnston, W.G., and Gilman, J.J., J. Appl. Phys., 30, 129 (1959).

13. Cottrell, A.H., Bristol Conf. on Strength of Solids, Phys. Soc. London, 30 (1948).

14. Fisher, J.C., and Rodgers, H.C., Acta Met., 4, 180 (1956).

15. Fisher, J.C., Trans. ASM, 47, 451 (1955).

16. Adams, M.A., and Iannucci, A., ASD Technical Report TR 61-203, Contract No. AF 33(616)-7173 (1961).

17. Murray, G.T., and Burn, R.A., ASD Technical Report TR 61-203, Contract No. AF 33(616)-7173, Part II (1962).

REFERENCES (Cont'd)

18. Adams, M.A., J. Sci. Instr., 36, 444 (1949).

19. DMIC Report 133, "Tantalum and Tantalum Alloys", Battelle Memorial Institute, Columbus, Ohio (July, 1960).

20. Tjerkstra, H.H., Acta Met., 9, 259 (1961).

21. Gilbert, A., Hull, D., Owen, W.S., and Reid, C.N., J. Less-Common Metals, 4, 399 (1962).

22. Wilcox, B.A., J. Less-Common Metals, 2, 292 (1960).

23. Lawley, A., Liebman, W., and Maddin, R., Acta Met., 9, 841 (1961).

24. Tedmon, C.S., and Ferriss, D.P., Trans. AIME, 224, 1079 (1962).

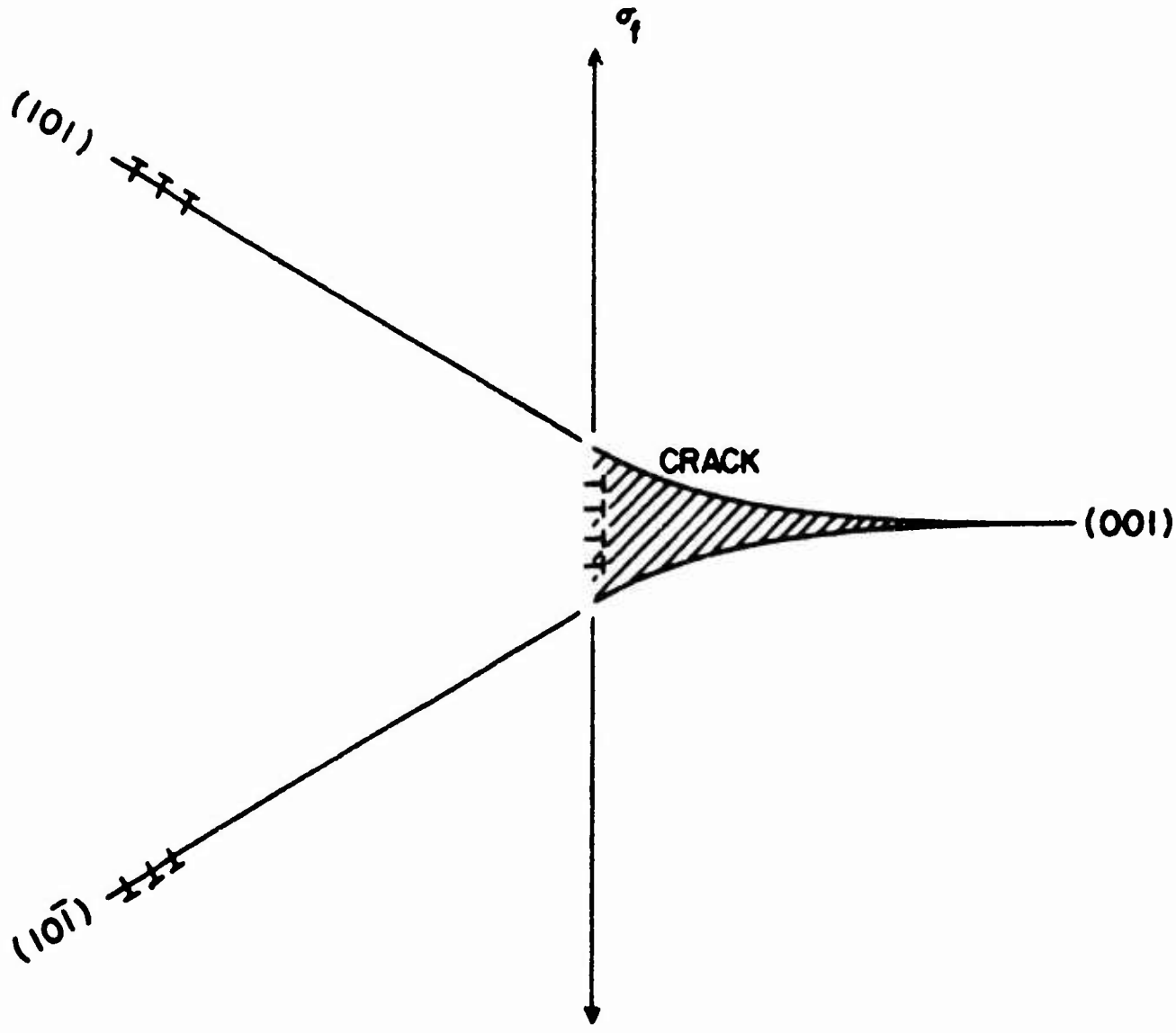

FIG. 1. COTTRELL MODEL FOR GENERATION OF A CLEAVAGE CRACK BY DISLOCATION PILE-UP AT INTERSECTING SLIP PLANES.

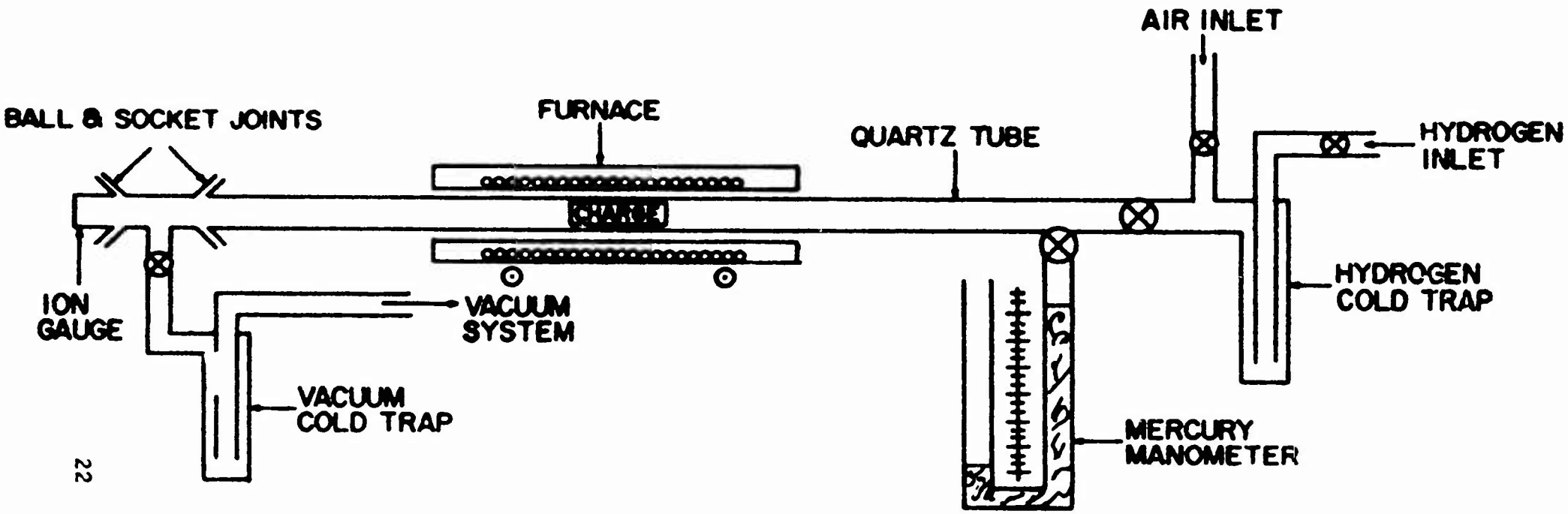

FIG. 2. SCHEMATIC DRAWING OF HYDROGEN CHARGING APPARATUS.

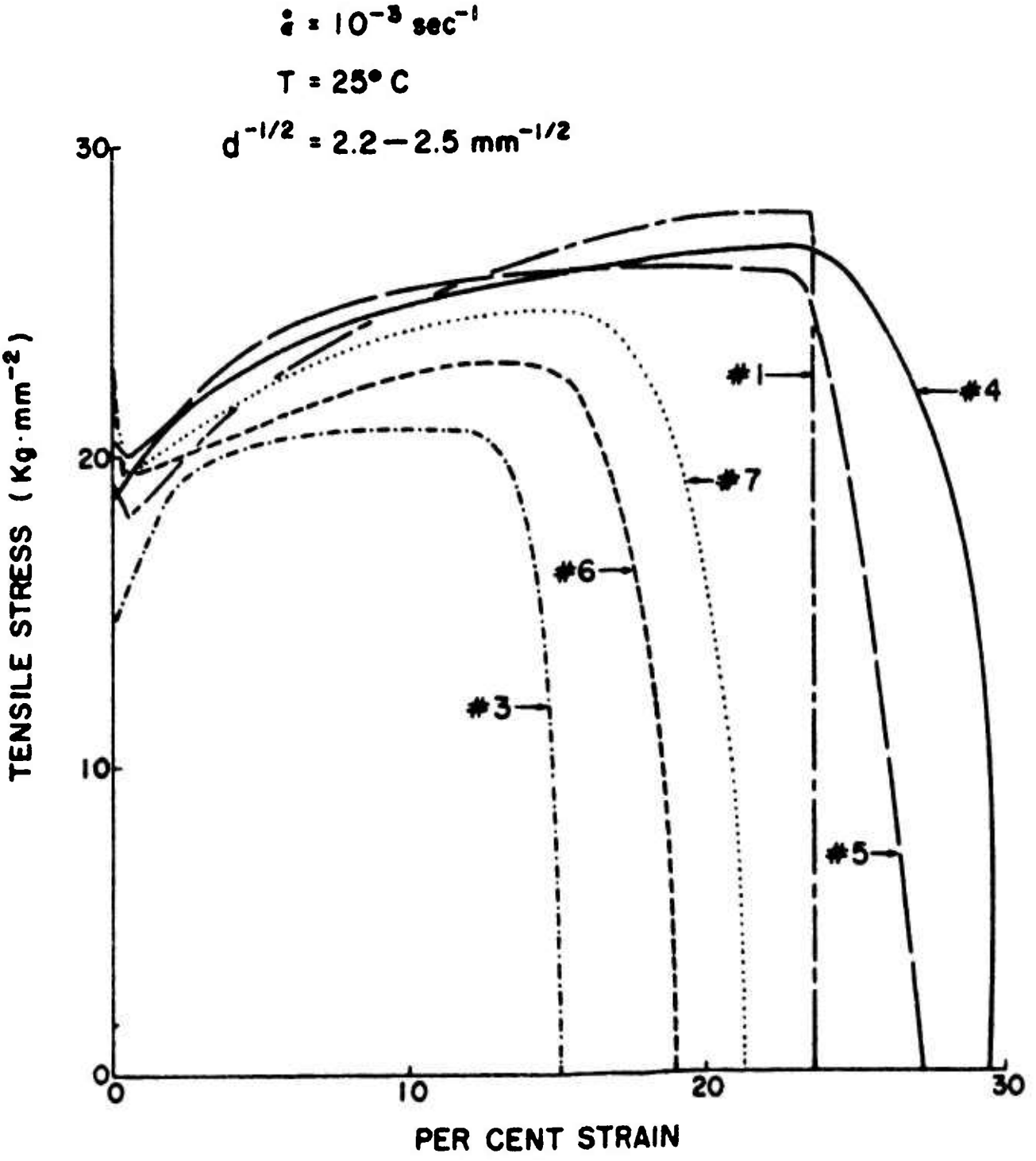

FIG. 3. TYPICAL TENSILE CURVES FOR Ta-H ALLOYS.

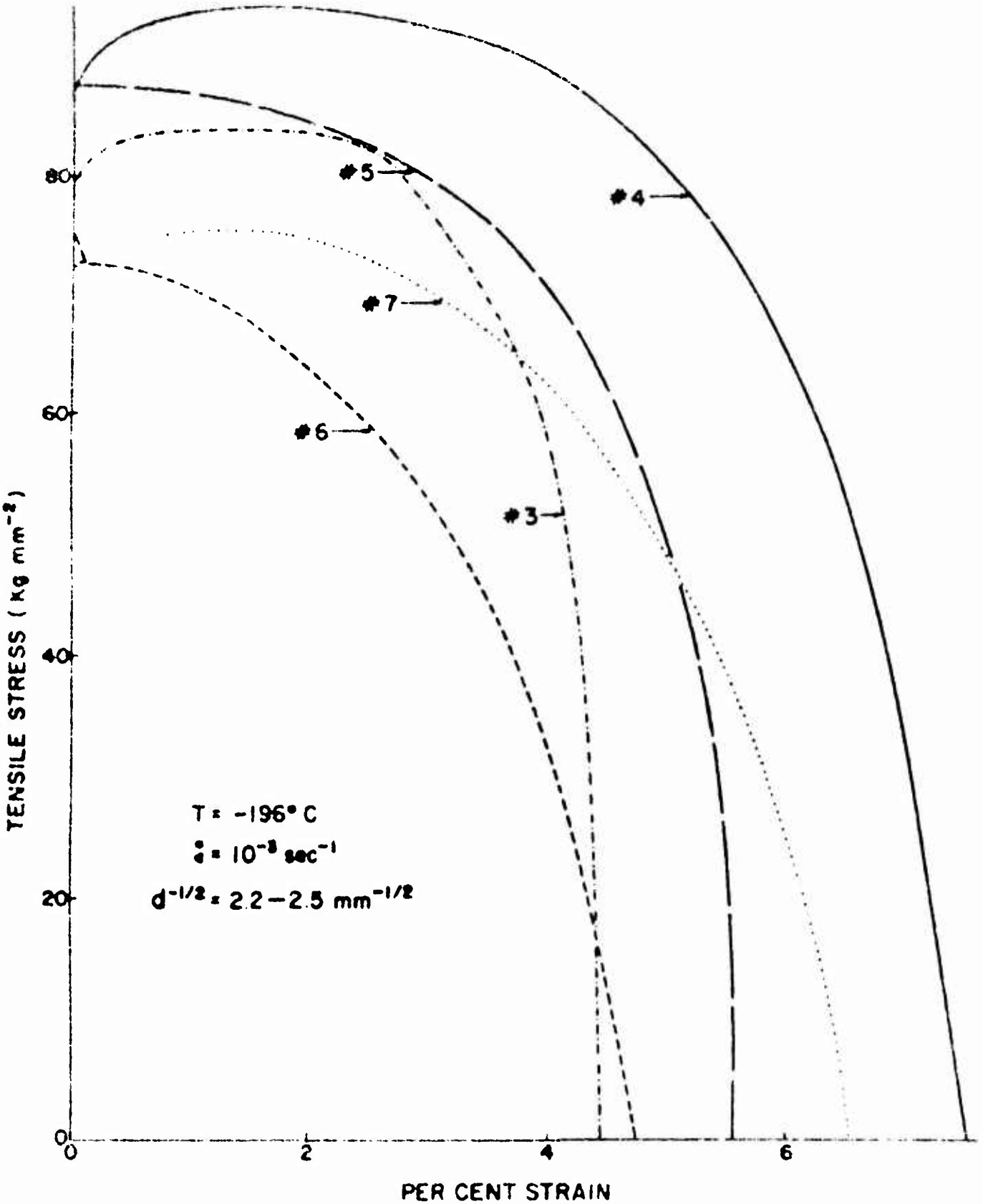

FIG 4 TYPICAL TENSILE CURVES FOR Ta-H ALLOYS

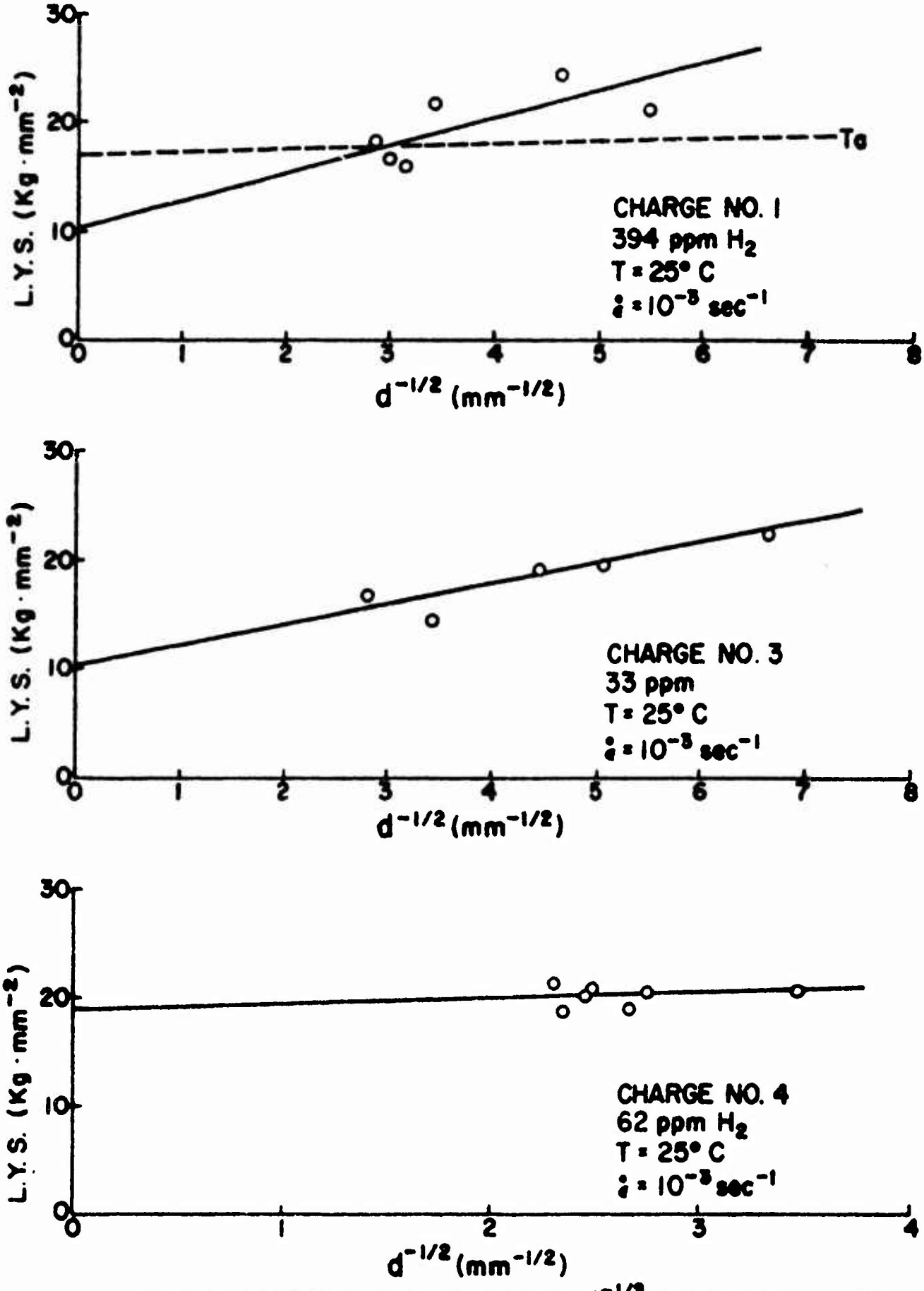

FIG. 5. LOWER YIELD STRESS VS. $d^{-1/2}$ FOR Ta-H ALLOYS.

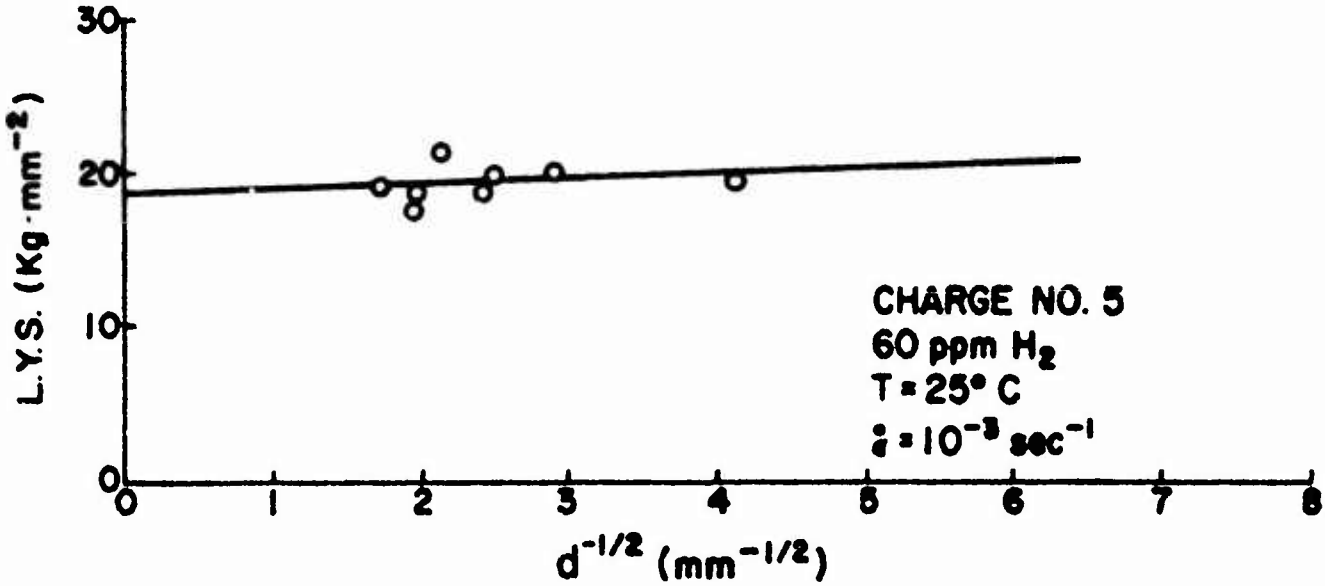

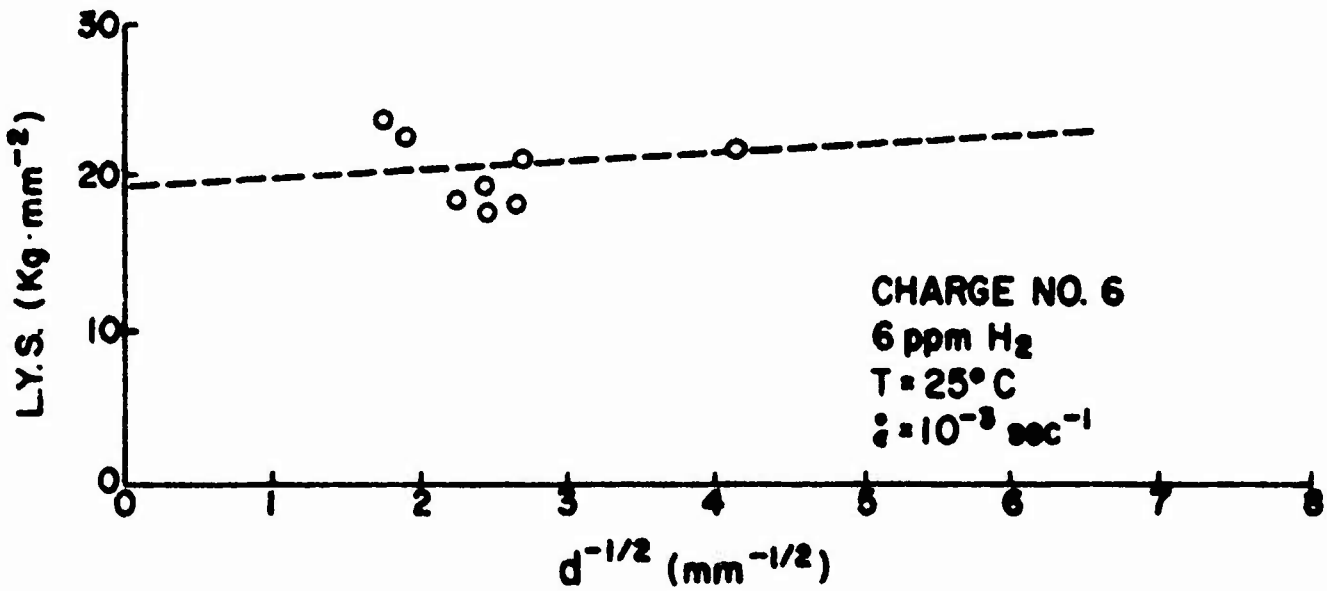

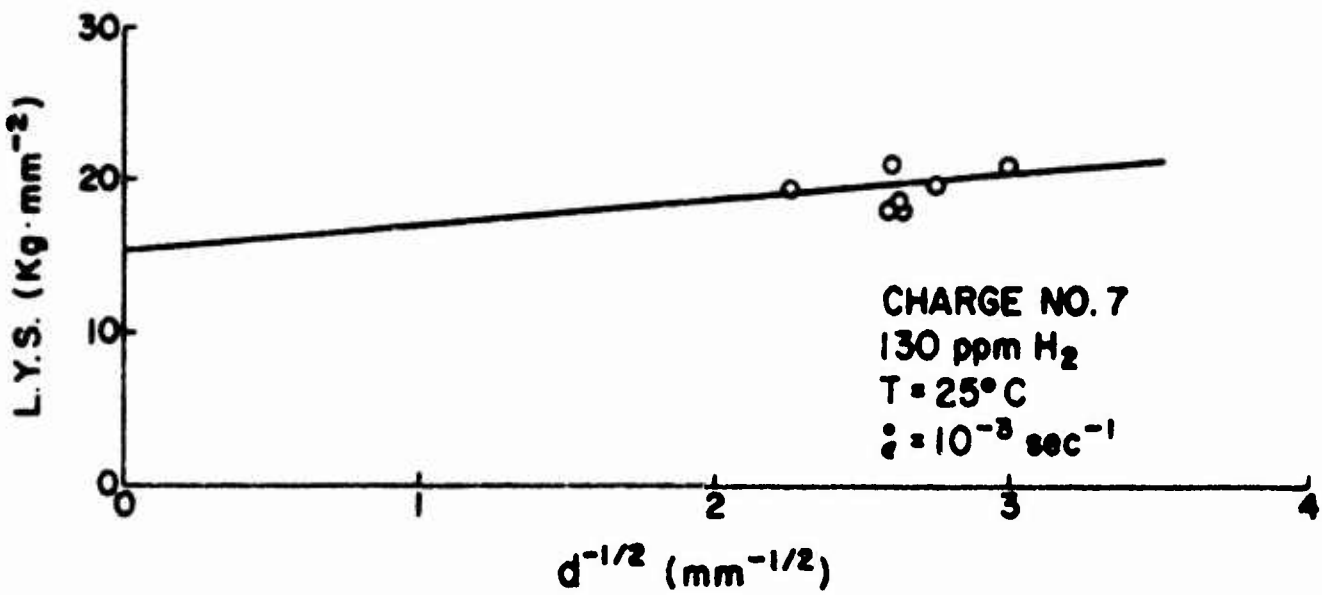

FIG. 5. (CONTINUED)

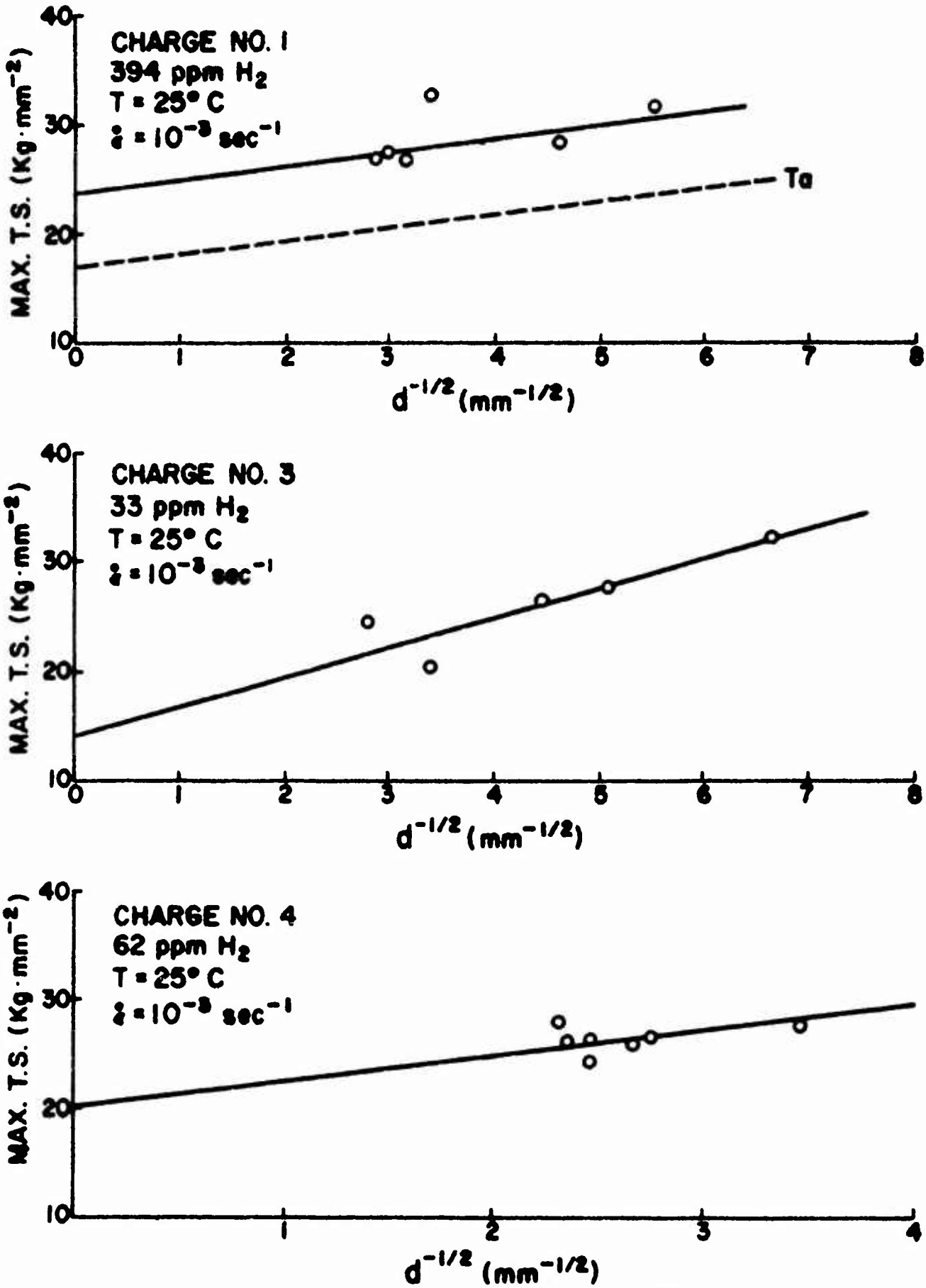

FIG. 6. MAXIMUM TENSILE STRESS VS. $d^{-1/2}$ FOR Ta-H ALLOYS.

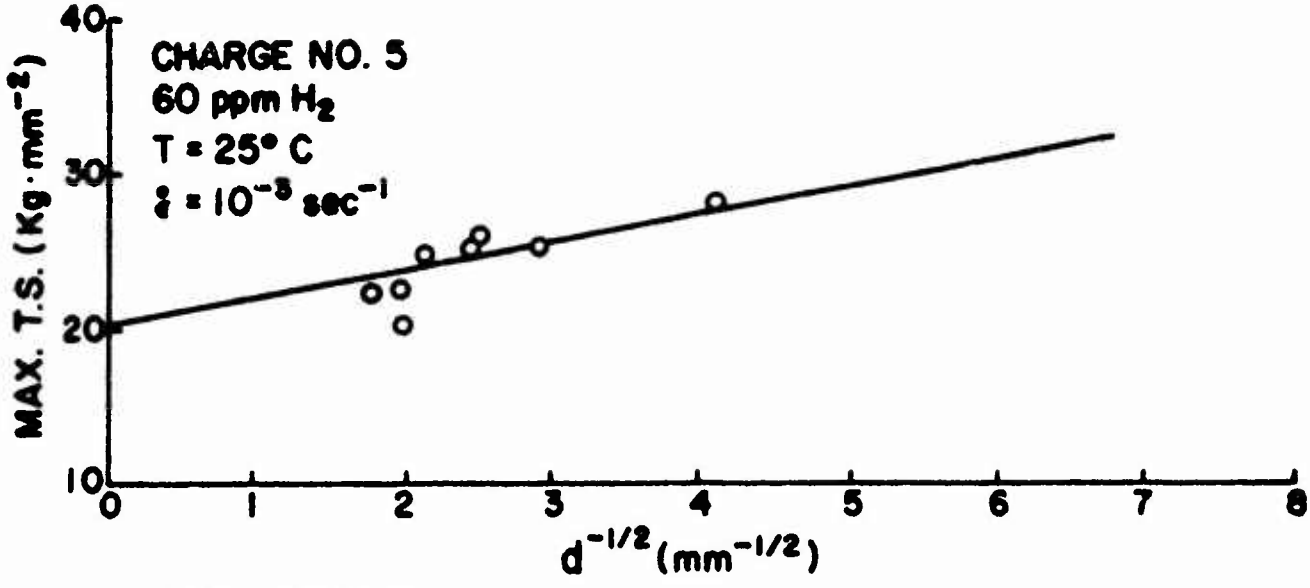

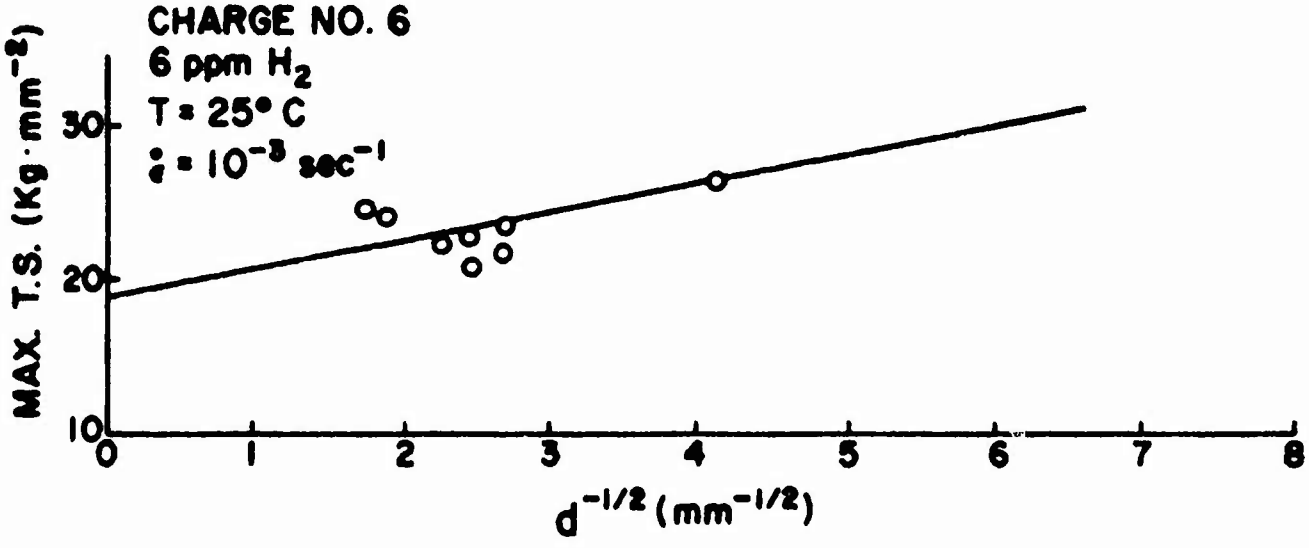

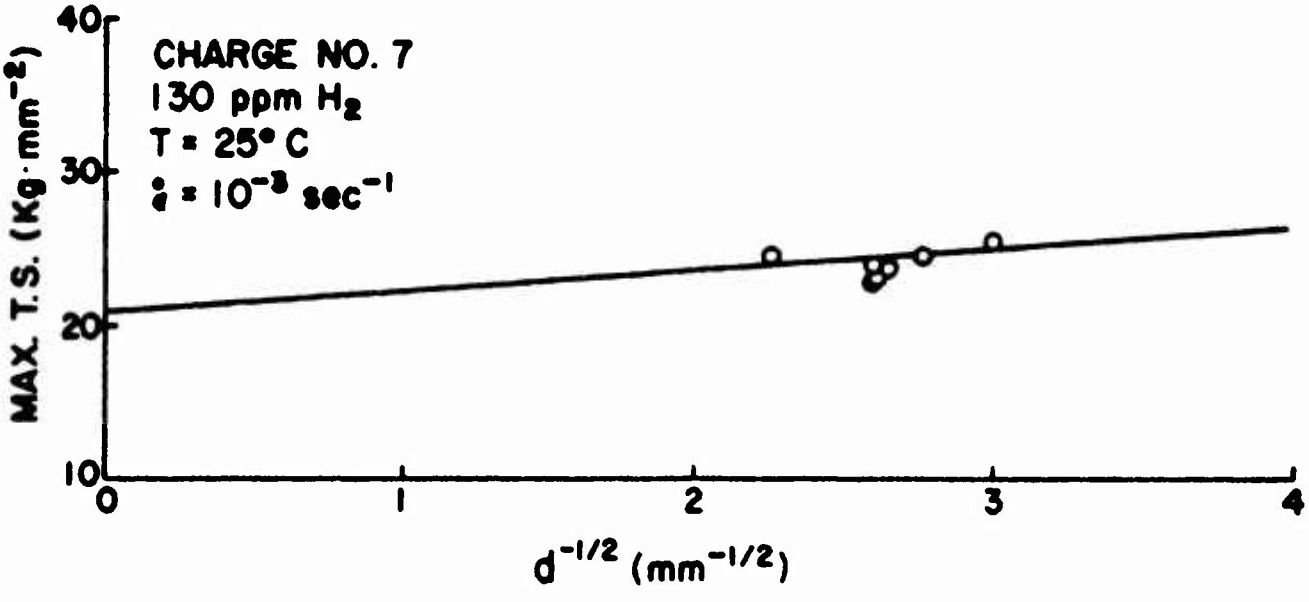

FIG. 6. (CONTINUED)

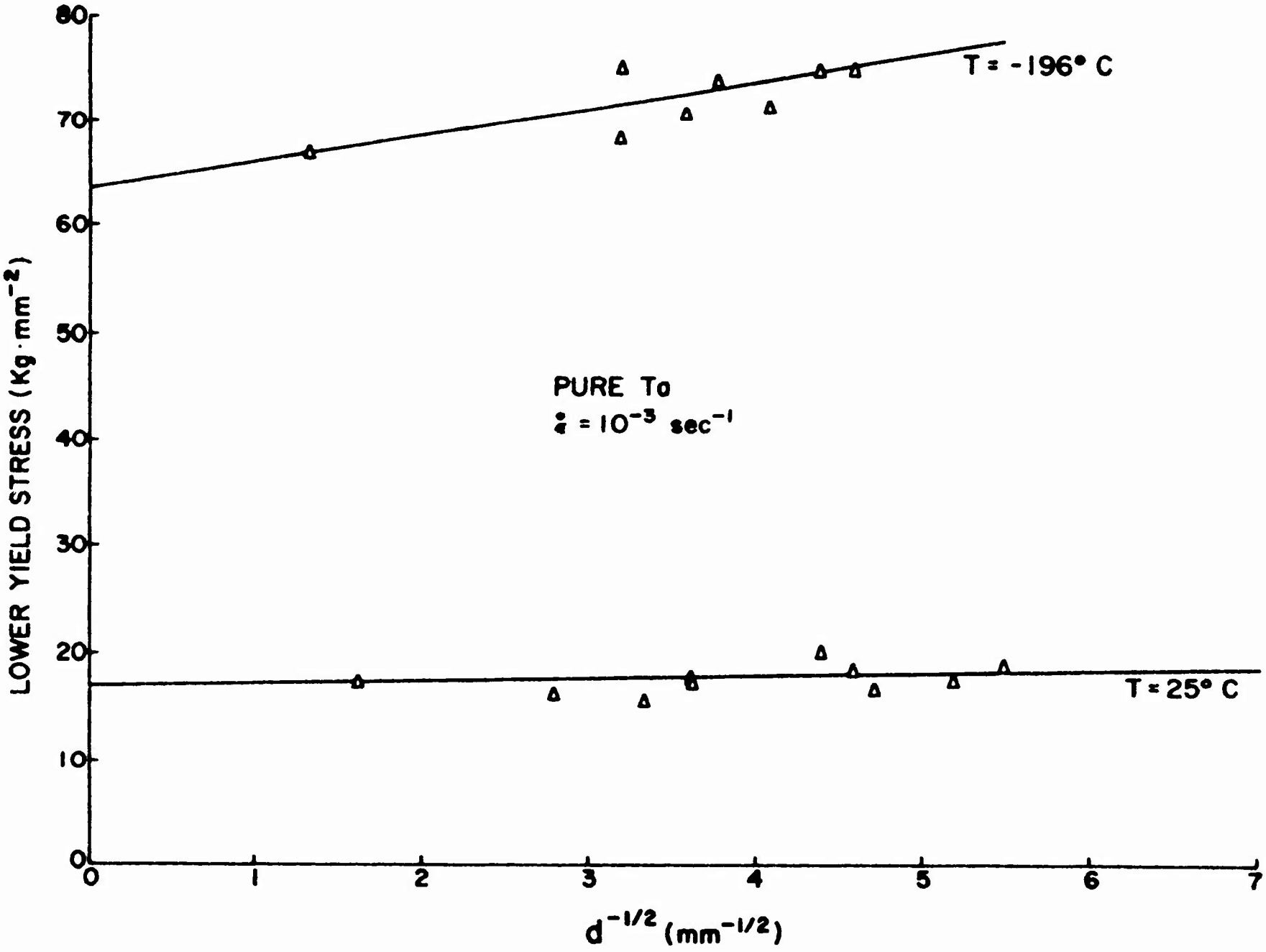

FIG. 7. LOWER YIELD STRESS VS. $d^{-1/2}$ FOR PURE TANTALUM.

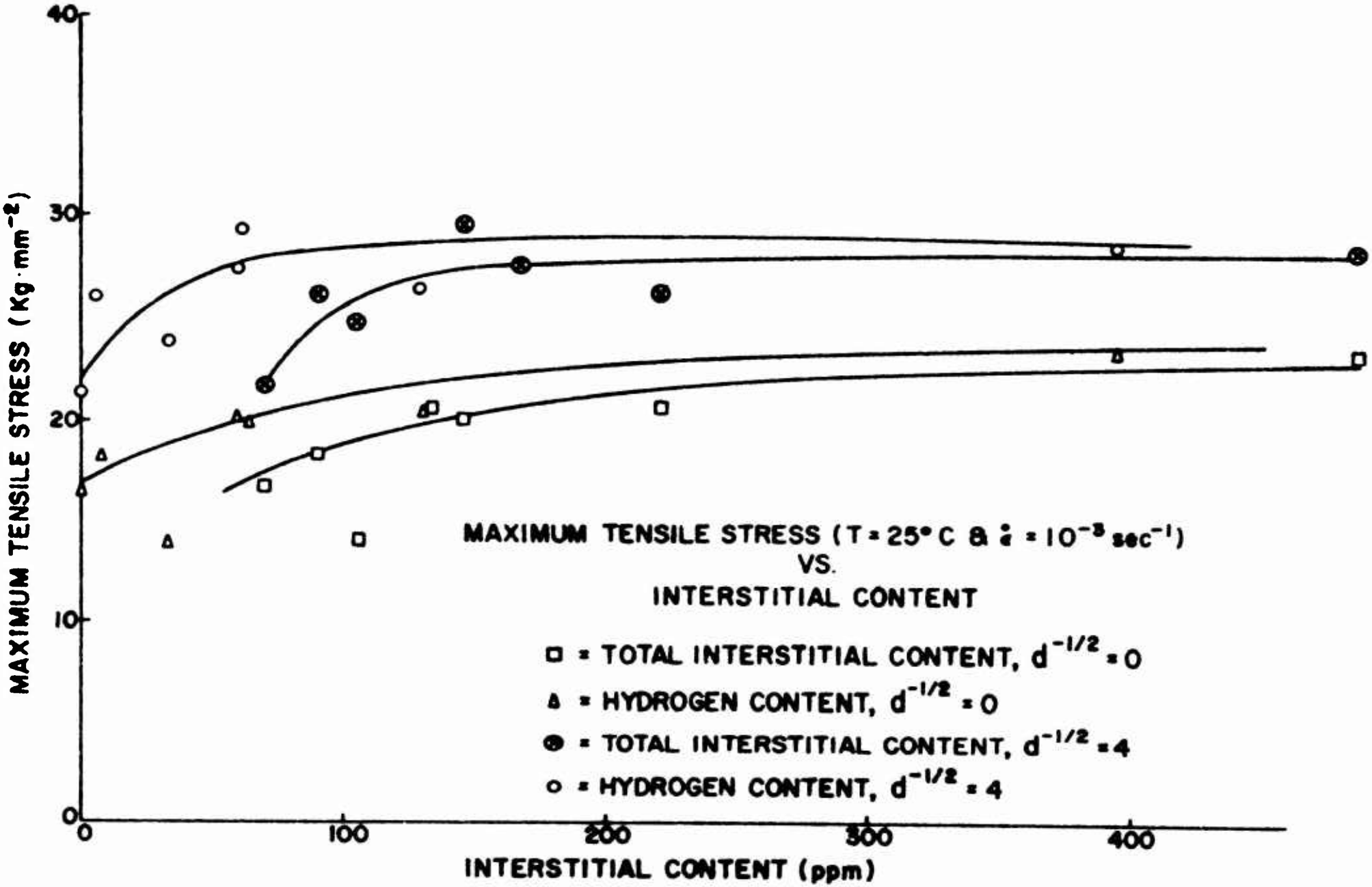

FIG. 8. MAXIMUM TENSILE STRESS VS. INTERSTITIAL CONTENT FOR Ta-H ALLOYS.

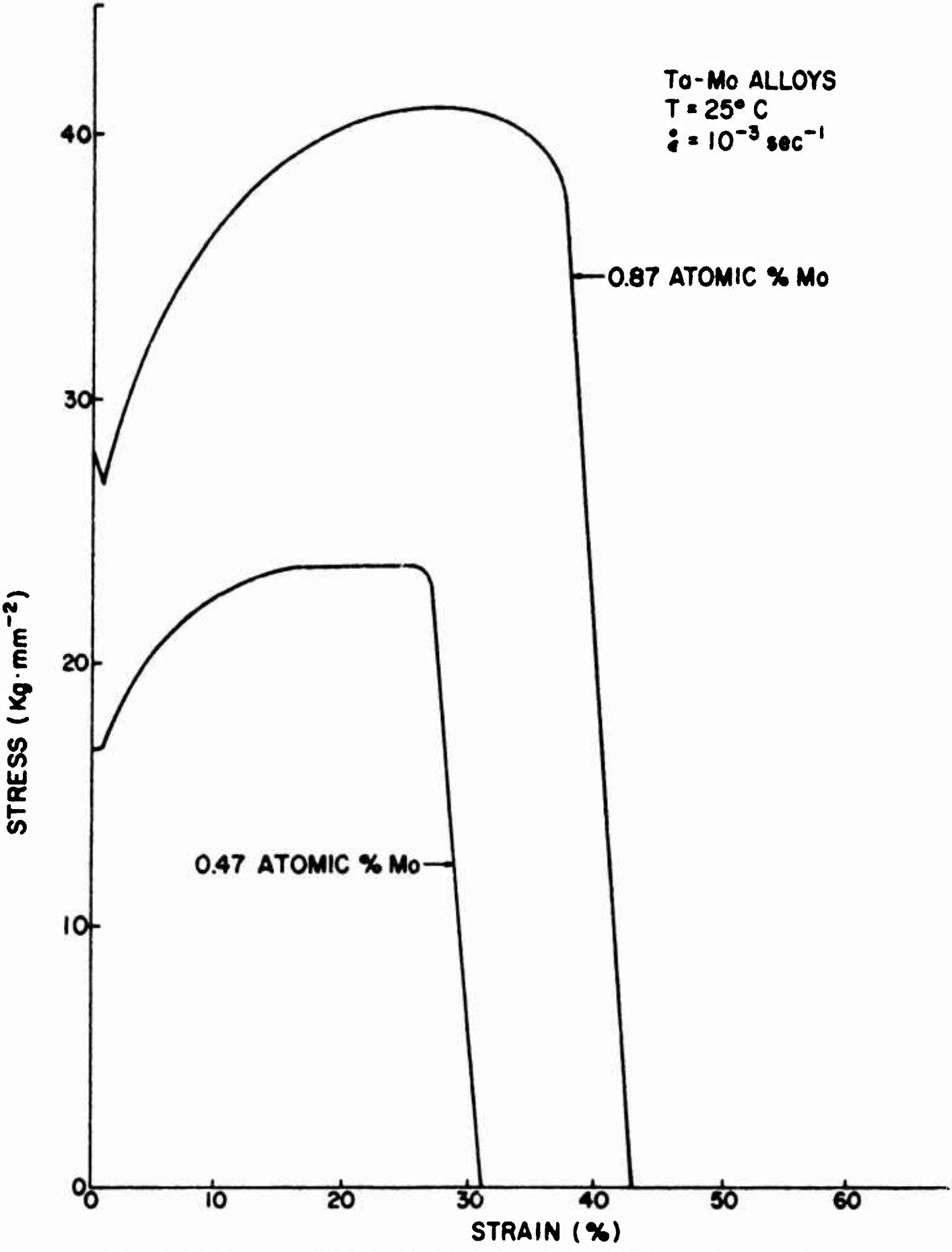

FIG. 9. TYPICAL 25° C TENSILE CURVES FOR Ta-Mo ALLOYS.

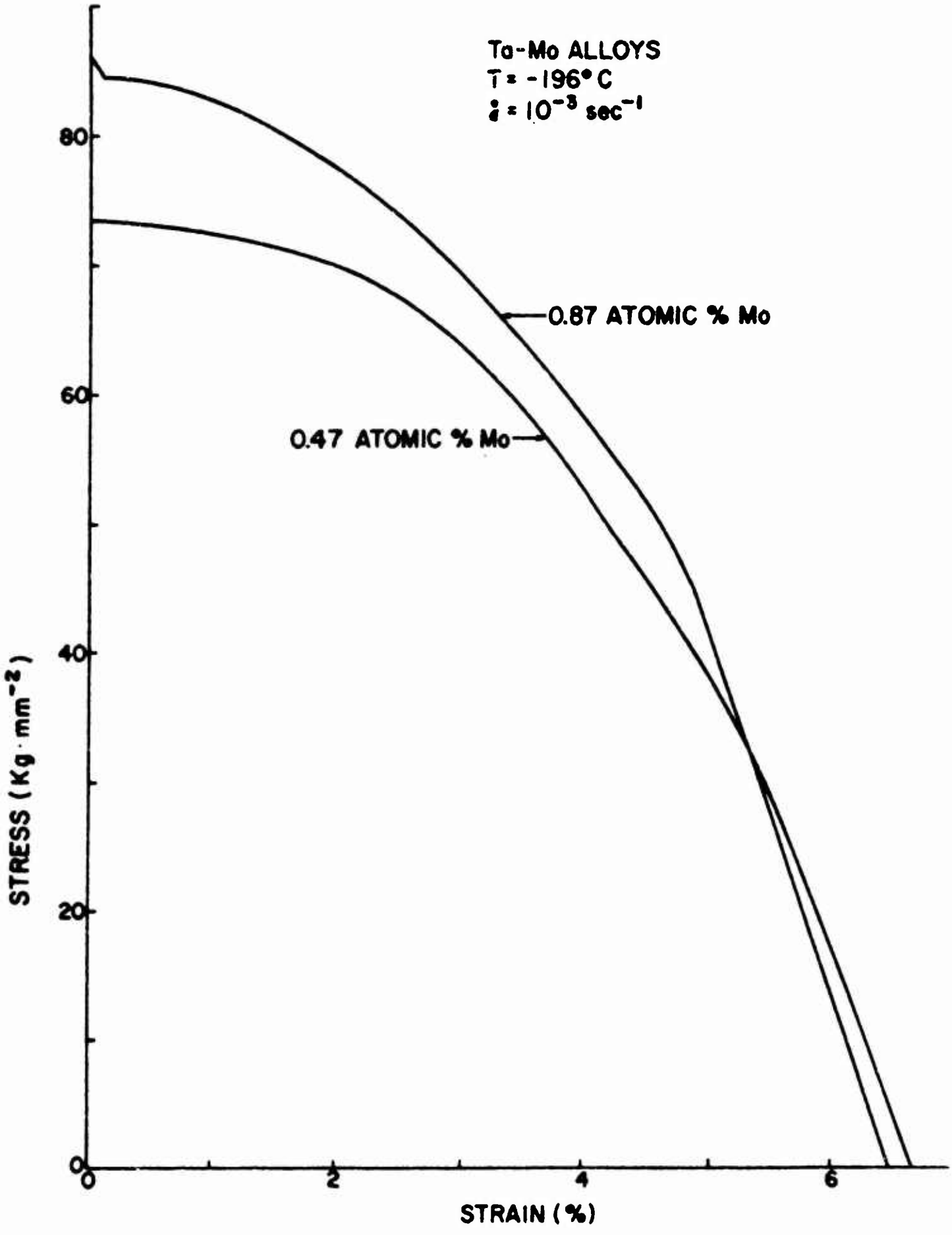

FIG. 10. TYPICAL -196° C TENSILE CURVES FOR Ta-Mo ALLOYS IN ABSENCE OF TWINNING.

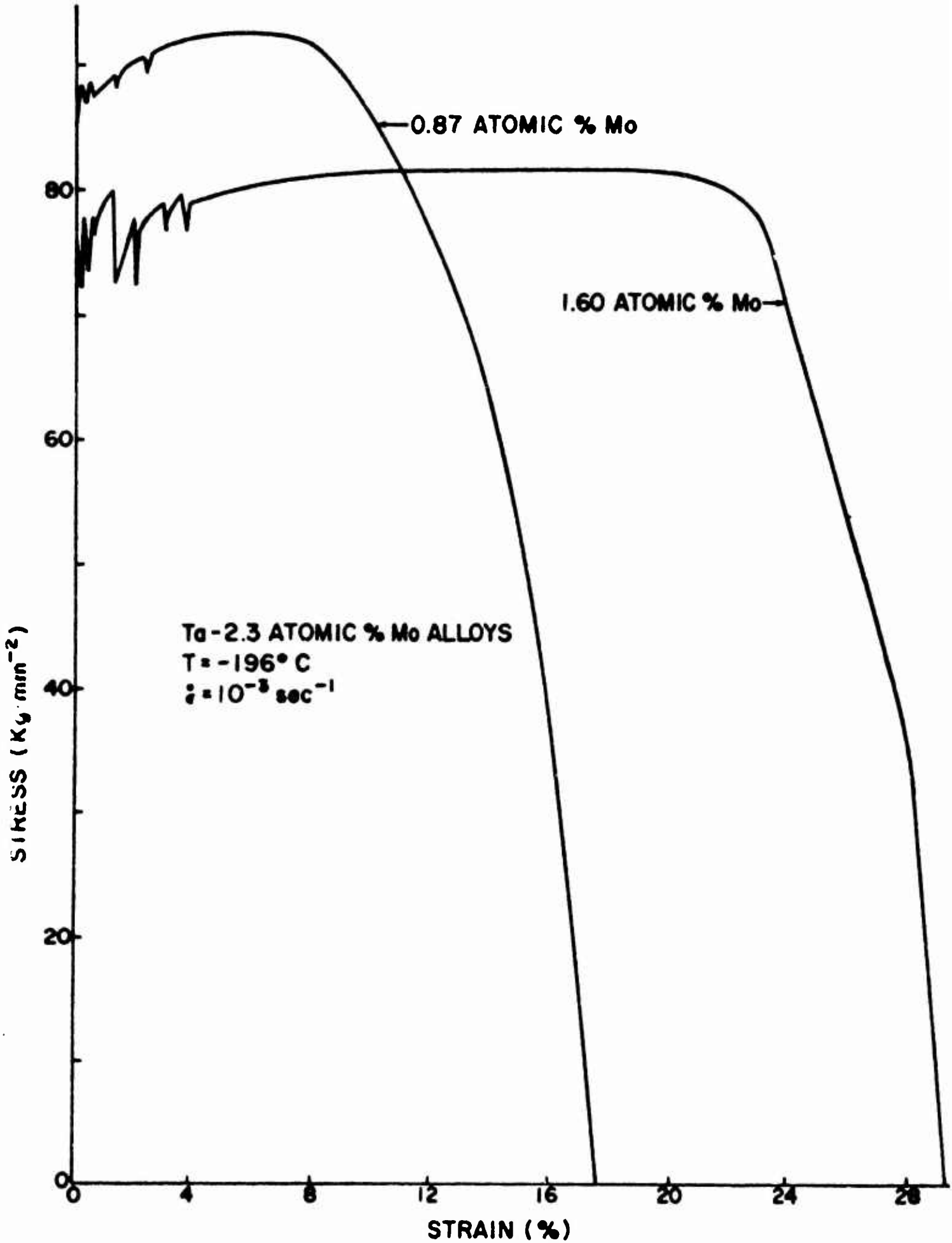

FIG. 11. TYPICAL TENSILE CURVES FOR Ta-Mo ALLOYS AT -196° C ILLUSTRATING TWINNING.

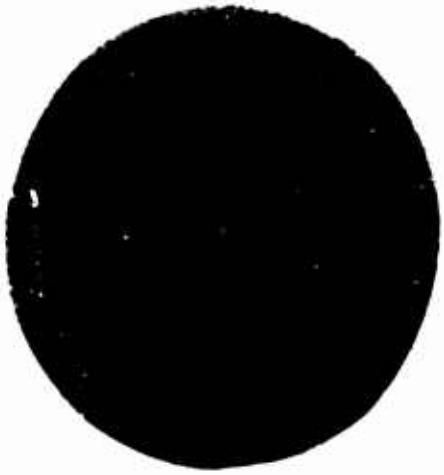

a

75X, $d^{-1/2} = 3.5$ $mm^{-1/2}$

b

75X, $d^{-1/2} = 7.0$ $mm^{-1/2}$

Typical Microstructures of Ta-Mo Alloys

c

200X, 1.6 at.% Mo

d

75X, 0.87 at.% Mo

Twinning in Ta-Mo Alloys Tested at -196°C

Fig. 12

e

50X, 25°C

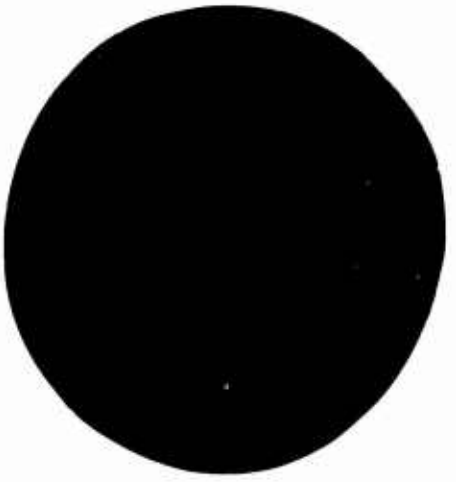

f

50X, -196°C

Fracture Modes of Ta-Mo Alloys

Fig. 12
(Continued)

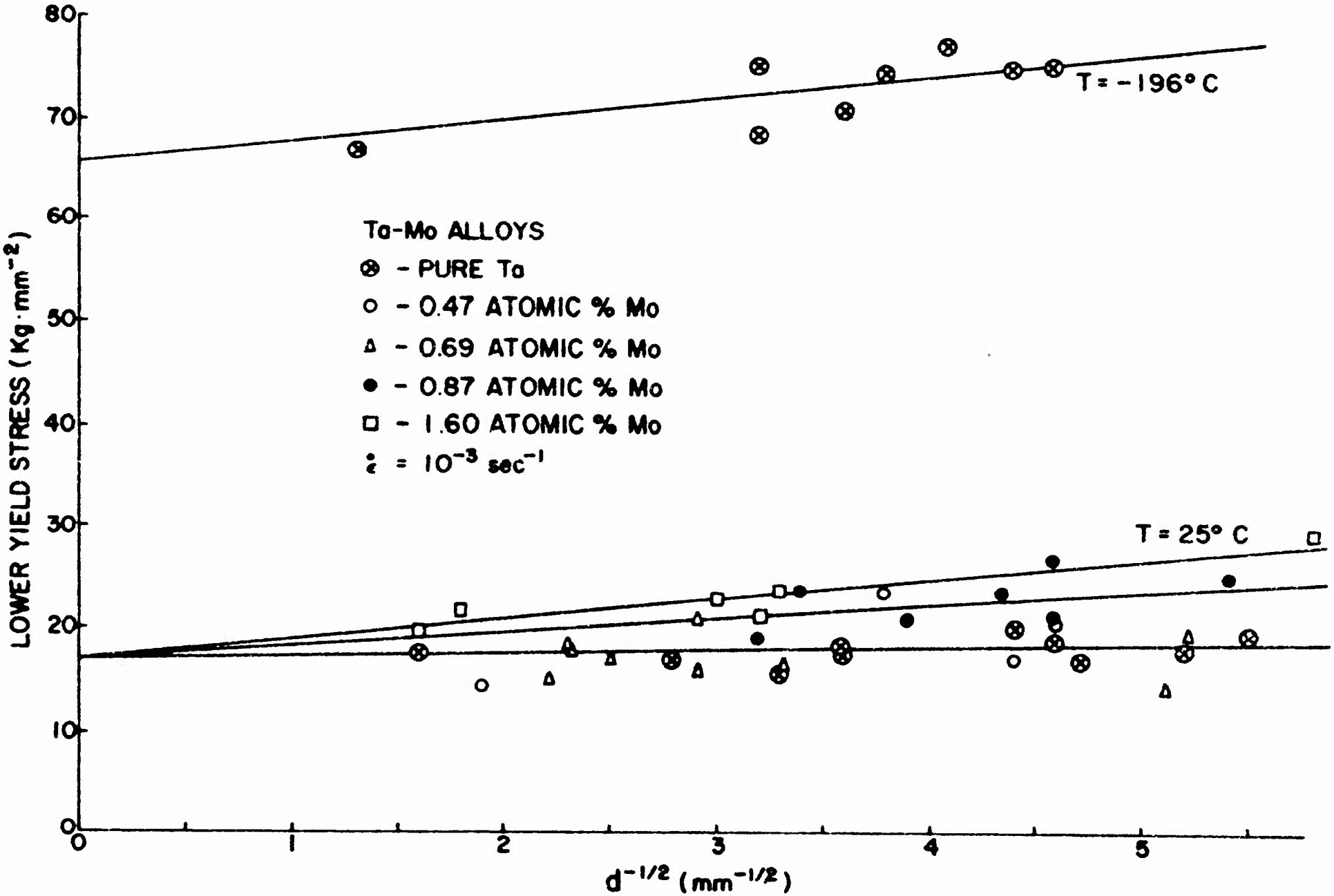

FIG. 13. LOWER YIELD STRESS VS. $d^{-1/2}$ FOR Ta AND Ta-Mo ALLOYS.

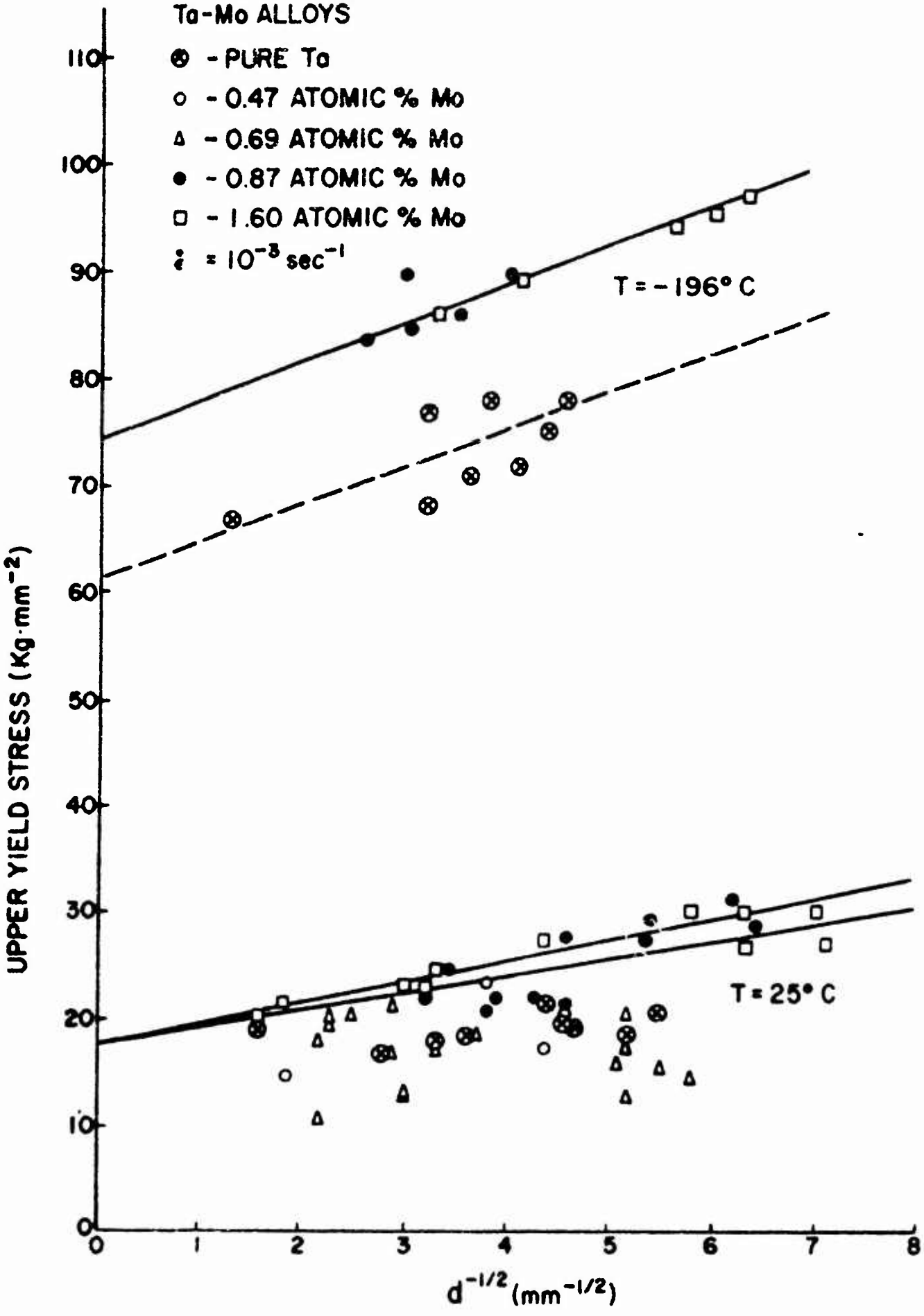

FIG. 14. UPPER YIELD STRESS VS. $d^{-1/2}$ FOR Ta AND Ta-Mo ALLOYS.

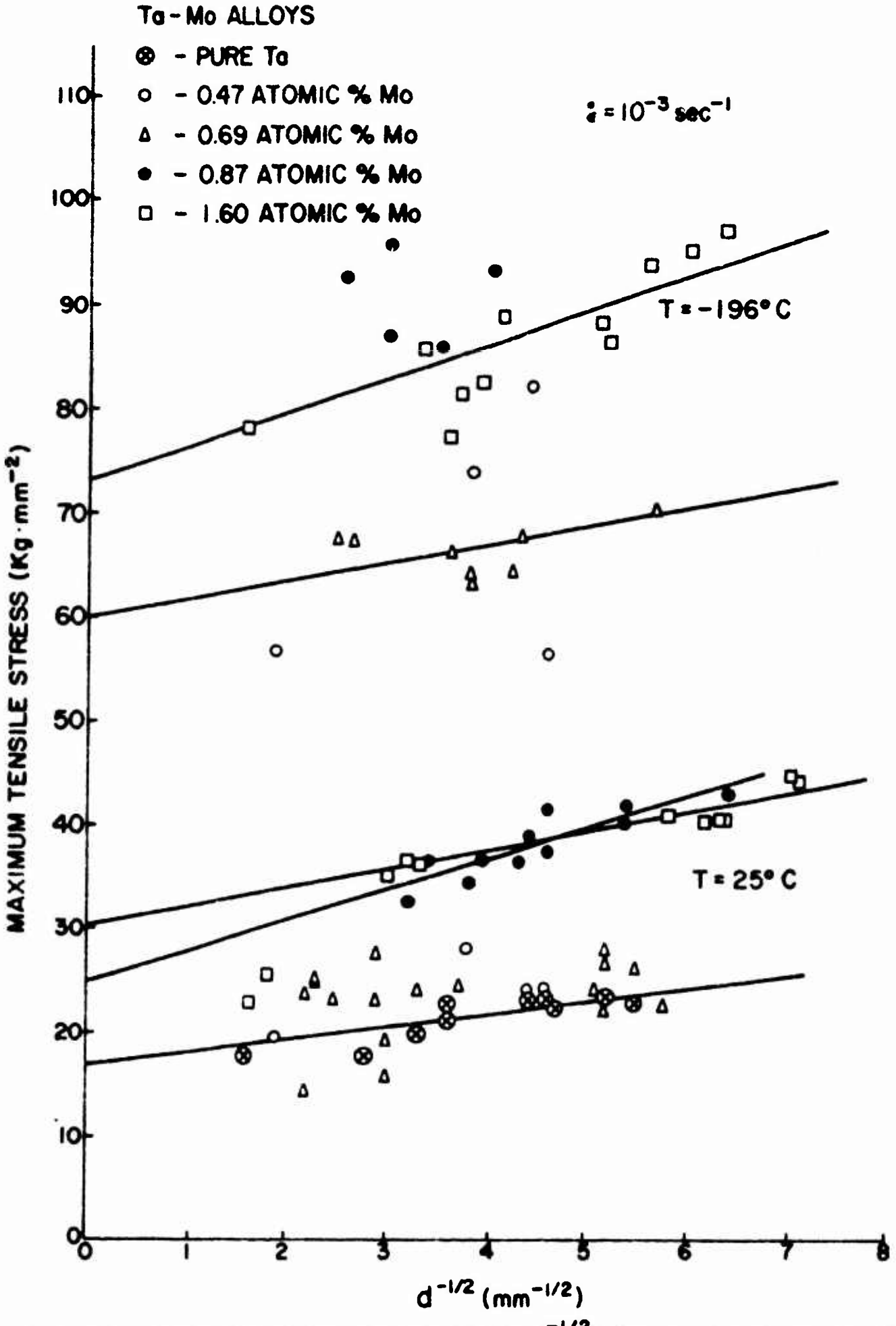

FIG. 15. MAXIMUM TENSILE STRESS VS. $d^{-1/2}$ FOR Ta AND Ta-Mo ALLOYS.

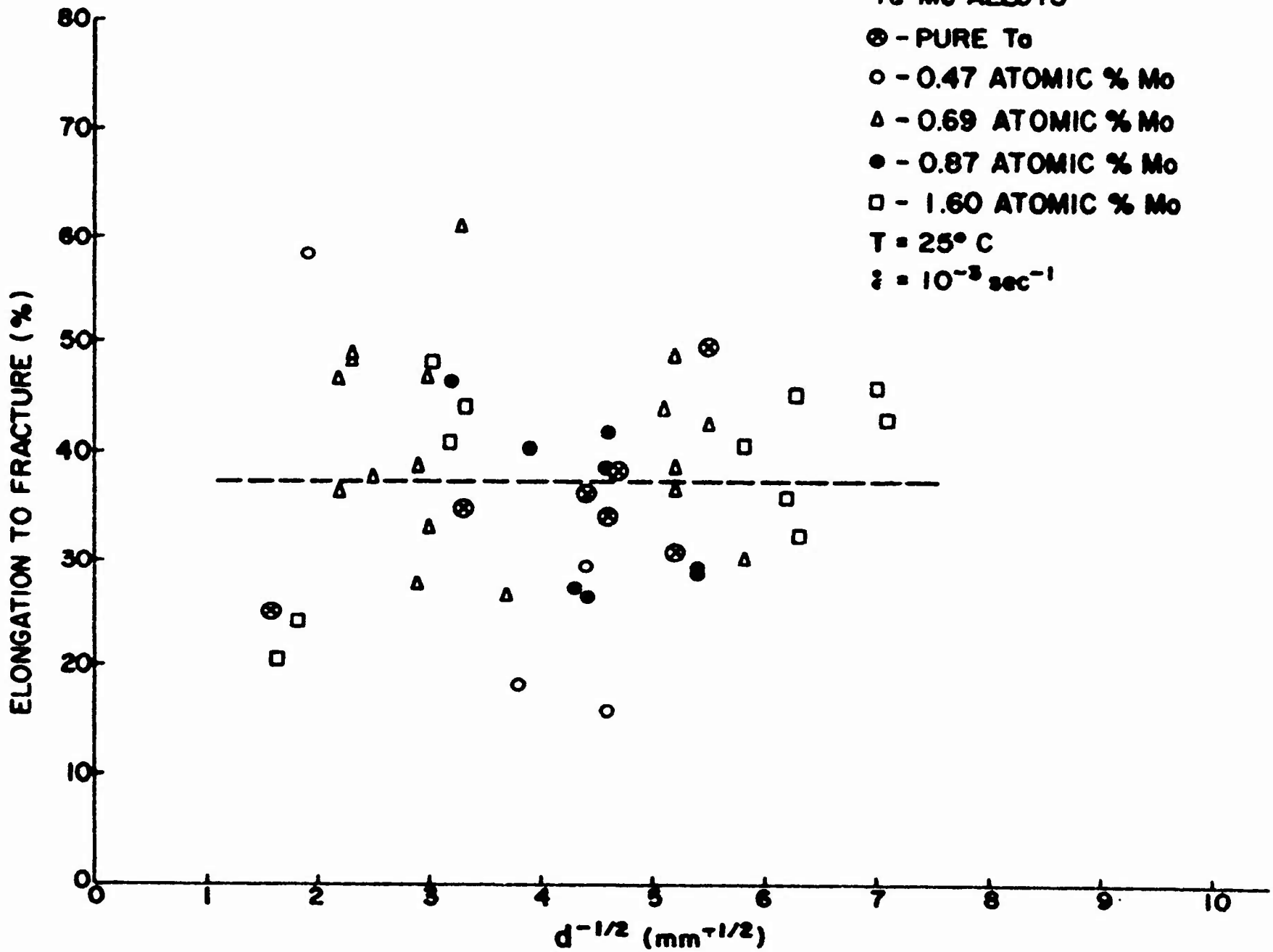

FIG. 16. ELONGATION TO FRACTURE VS. $d^{-1/2}$ FOR Ta AND Ta-Mo ALLOYS.

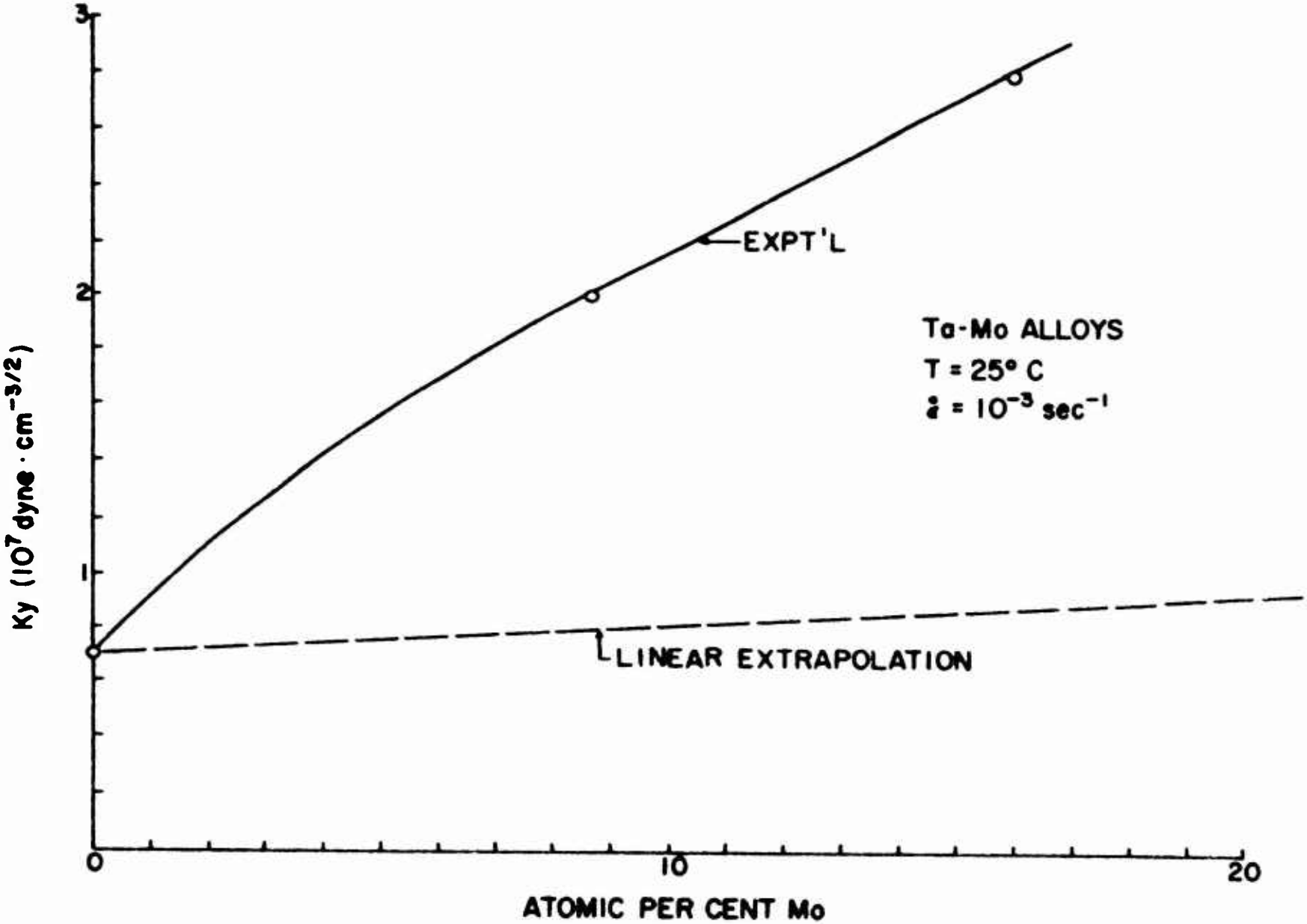

FIG. 17. Ky VS. Mo CONTENT FOR DILUTE Ta-Mo ALLOYS.

TABLE I

CHEMICAL ANALYSIS OF "AS-RECEIVED"

TANTALUM

Impurity Element	As-Received ppm (Average)
O_2	150
N_2	100
H_2	2
C	50
Nb	$<$ 300
Fe	50
Ti	30
Si	80
Al	50

TABLE II

TENSILE DATA FOR Ta-H ALLOYS

CHARGE NO. 1

Spec. No.	Test Temp. (°C)	$d^{-1/2}$ ($mm^{-1/2}$)	L.Y.S. ($Kg.mm^{-2}$)	U.Y.S. ($Kg.mm^{-2}$)	Max. Tensile Stress ($Kg.mm^{-2}$)	Unif. Elong. (%)	Total Elong. (%)
1	25	5.50	21.4	21.4	31.7	23.6	23.6
2	25	4.60	24.4	24.4	28.5	4.0	4.0
3	25	3.40	21.8	21.8	32.7	14.7	14.7
4	25	3.17	16.0	16.7	26.8	29.0	29.0
5	25	2.88	18.1	19.1	26.9	23.4	23.4
6	25	2.98	16.7	17.8	27.5	27.2	27.2

TABLE II

(CONTINUED)

CHARGE NO. 3

Test Spec.	Test Temp. (°C)	$d^{-1/2}$ ($mm^{-1/2}$)	L.Y.S. ($Kg.mm^{-2}$)	U.Y.S. ($Kg.mm^{-2}$)	Max. Tensile Stress ($Kg.mm^{-2}$)	Unif. Elong. (%)	Total Elong. (%)
1	25	6.66	22.4	22.4	32.5	22.3	23.9
2	25	5.08	19.6	19.6	27.8	18.6	20.5
3	25	4.43	19.2	19.2	26.9	10.4	11.3
4	25	2.80	16.7	16.7	24.6	15.2	16.5
5	25	3.42	14.5	14.5	20.1	12.8	14.4
6	-196	5.08	-	86.5	90.2	1.4	2.7
7	-196	4.64	-	84.5	86.5	1.1	2.6
8	-196	5.42	-	91.6	96.5	1.5	2.8
9	-196	4.63	-	86.9	91.6	1.3	2.4
10	-196	3.55	-	83.0	87.3	1.9	2.7
11	-196	3.50	-	80.3	83.5	2.6	4.3
12	-196	3.33	-	78.2	80.3	1.6	3.2

TABLE II

(CONTINUED)

CHARGE NO. 4

Spec. No.	Test Temp. (°C)	$d^{-1/2}$ ($mm^{-1/2}$)	L.Y.S. ($Kg.mm^{-2}$)	U.Y.S. ($Kg.mm^{-2}$)	Max. Tensile Stress ($Kg.mm^{-2}$)	Unif. Elong (%)	Total Elong. (%)
1	-196	2.34	-	-	82.7	-	3.4
2	25	2.31	23.5	23.5	28.0	10.8	14.9
3	-196	3.16	-	-	92.0	-	5.8
4	25	2.46	19.6	20.0	24.3	31.6	34.6
5	25	2.66	19.1	19.2	25.7	21.8	24.5
6	-196	2.46	-	75.2	81.0	3.0	6.3
7	25	2.34	18.7	18.7	26.4	24.4	28.6
8	25	2.75	20.4	20.6	26.8	16.8	19.9
9	-196	2.50	-	88.0	93.6	2.2	6.1
10	-196	4.00	-	-	97.1	-	6.4
11	-196	2.81	-	82.2	87.0	3.0	6.9
12	25	2.46	20.0	20.3	26.6	13.5	17.8
13	-196	2.56	-	-	95.7	-	5.0
14	-196	2.56	-	78.7	91.4	2.8	4.4
15	25	3.48	20.2	20.4	27.7	14.8	17.0

TABLE II

(CONTINUED)

CHARGE NO. 5

Spec. No.	Test Temp. (°C)	$d^{-1/2}$ ($mm^{-1/2}$)	L.Y.S. ($Kg.mm^{-2}$)	U.Y.S. ($Kg.mm^{-2}$)	Max. Tensile Stress ($Kg.mm^{-2}$)	Unif. Elong. (%)	Total Elong. (%)
1	-196	2.46	-	-	89.5	-	4.4
2	25	2.12	21.8	23.0	24.9	12.1	15.2
3	-196	2.85	-	80.0	86.7	2.2	5.0
4	25	2.50	20.1	20.5	26.0	23.1	26.4
5	25	1.77	19.4	20.6	22.5	16.3	22.8
6	-196	2.34	-	76.6	81.8	1.9	5.2
7	25	2.91	20.3	20.4	25.3	11.9	15.1
8	-196	2.25	-	81.0	81.4	1.0	3.4
9	25	2.43	18.8	19.0	25.6	21.5	23.8
10	25	1.99	18.7	19.5	22.6	12.7	15.9
11	25	1.99	17.5	18.2	20.1	10.6	13.5
12	-196	2.56	-	74.6	77.0	1.0	2.6
13	-196	2.21	-	-	87.7	-	4.5
14	-196	2.88	-	82.2	85.3	1.4	3.6
15	25	4.11	19.5	20.1	28.2	24.1	28.6

TABLE II

(CONTINUED)

CHARGE NO. 6

Spec. No.	Test Temp. (°C)	$d^{-1/2}$ ($mm^{-1/2}$)	L.Y.S. ($Kg.mm^{-2}$)	U.Y.S. ($Kg.mm^{-2}$)	Max. Tensile Stress ($Kg.mm^{-2}$)	Unif. Elong. (%)	Total Elong. (%)
1	-196	2.12	-	-	77.2	-	3.9
2	25	2.66	21.3	23.7	23.7	16.3	19.7
3	25	4.11	21.9	25.0	26.4	13.4	18.6
4	-196	2.12	-	-	80.6	-	4.0
5	25	2.25	18.5	21.8	22.3	18.9	24.0
6	25	1.74	23.9	23.3	24.6	7.5	13.0
7	25	1.87	22.5	22.9	24.2	9.2	14.7
8	-196	2.25	-	-	75.0	-	3.1
9	25	2.43	19.4	22.8	22.7	15.1	18.4
10	25	2.66	18.2	22.5	21.9	21.7	26.1
11	25	2.43	18.1	21.7	20.8	21.0	26.2
12	-196	2.46	-	-	74.3	-	3.9
13	-196	1.99	-	-	81.2	-	3.1
14	-196	3.20	-	-	89.7	-	2.9
15	-196	1.67	-	-	88.4	-	3.9

TABLE II

(CONTINUED)

CHARGE NO. 7

Spec. No.	Test Temp. (°C)	$d^{-1/2}$ ($mm^{-1/2}$)	L.Y.S. ($Kg.mm^{-2}$)	U.Y.S. ($Kg.mm^{-2}$)	Max. Tensile Stress ($Kg.mm^{-2}$)	Unif. Elong. (%)	Total Elong. (%)
1	-196	2.53	-	79.5	81.4	1.2	4.8
2	-196	2.40	-	-	81.3	-	5.7
3	-196	2.81	-	54.8	73.1	3.1	6.3
4	-196	2.94	-	76.7	79.6	1.7	3.9
5	-196	2.43	-	73.6	76.8	1.8	5.8
6	25	2.75	19.7	22.2	24.6	14.6	18.2
7	25	2.59	17.9	21.3	22.9	18.7	23.2
8	25	2.62	17.9	20.2	23.5	25.0	29.4
9	25	2.25	19.4	22.0	24.6	16.2	21.8
10	25	2.59	17.7	20.8	23.1	20.7	23.3
11	25	2.59	21.0	22.6	24.0	10.5	14.4
12	25	3.00	21.0	23.8	25.3	19.7	23.6

TABLE III

TENSILE DATA FOR Ta-Mo ALLOYS

ALLOY NO. 1

Spec. No.	Test Temp. (°C)	$d^{-1/2}$ ($mm^{-1/2}$)	L.Y.S. ($Kg.mm^{-2}$)	U.Y.S. ($Kg.mm^{-2}$)	Max. Tensile Stress ($Kg.mm^{2}$)	Unif. Elong. (%)	Total Elong. (%)
1	25	1.9	14.7	14.7	19.7	54.2	58.4
2	25	3.8	23.5	23.5	28.3	11.6	18.5
3	25	4.4	17.2	17.2	24.4	26.1	29.7
4	25	4.6	20.4	20.7	24.4	11.3	15.5
5	-196	1.9	-	-	57.2	-	7.3
6	-196	3.8	-	-	74.0	-	6.4
7	-196	4.4	-	73.5	82.3	3.8	9.5
8	-196	4.6	-	54.8	56.4	1.9	6.0

TABLE III

(CONTINUED)

ALLOY NO. 2

Spec. No.	Test Temp. (°C)	$d^{-1/2}$ ($mm^{-1/2}$)	L.Y.S. ($Kg.mm^{-2}$)	U.Y.S. ($Kg.mm^{-2}$)	Max. Tensile Stress ($Kg.mm^{-2}$)	Unif. Elong. (%)	Total Elong. (%)
1	25	5.2	-	12.7	22.4	33.6	39.2
2	25	5.8	-	14.4	22.8	22.6	30.3
3	25	5.1	14.7	16.3	24.7	31.4	44.2
4	25	3.7	-	18.7	24.9	19.4	26.9
5	25	5.5	-	15.5	26.6	33.3	42.7
6	25	5.2	19.9	20.6	28.1	27.2	36.9
7	25	5.2	-	17.4	27.0	38.4	49.0
8	25	3.0	-	12.7	19.5	40.5	47.0
9	25	2.9	16.2	17.0	23.7	27.1	38.8
10	25	3.3	16.3	17.2	24.4	49.4	61.5
11	25	2.2	-	10.5	14.8	33.5	37.1
12	25	2.5	17.0	20.7	23.7	31.4	38.1
13	25	3.0	-	12.8	15.8	26.4	33.3
14	25	2.2	15.1	18.4	23.7	37.5	47.0
15	25	2.3	17.8	20.5	25.2	35.6	48.5
16	25	2.9	21.3	21.5	27.9	18.3	28.1

TABLE III

(CONTINUED)

ALLOY NO. 2

Spec. No.	Test Temp. (°C)	$d^{-1/2}$ ($mm^{-1/2}$)	L.Y.S. ($Kg.mm^{-2}$)	U.Y.S. ($Kg.mm^{-2}$)	Max. Tensile Stress ($Kg.mm^{-2}$)	Unif. Elong. (%)	Total Elong. (%)
17	25	2.3	18.7	19.5	25.3	36.4	49.1
18	-196	3.8	-	-	64.6	-	12.0
19	-196	5.7	-	-	70.4	-	11.6
20	-196	3.6	-	-	66.5	-	7.4
21	-196	3.8	-	-	63.5	-	18.3
22	-196	4.2	-	-	64.7	-	12.1
23	-196	4.3	-	-	68.2	-	9.6
24	-196	2.5	-	-	68.0	-	12.9
25	-196	2.6	-	-	68.2	-	11.8

TABLE III

(CONTINUED)

ALLOY NO. 3

Spec. No.	Test Temp. (°C)	$d^{-1/2}$ ($mm^{-1/2}$)	L.Y.S. ($Kg.mm^{-2}$)	U.Y.S. ($Kg.mm^{-2}$)	Max. Tensile Stress ($Kg.mm^{-2}$)	Unif. Elong. (%)	Total Elong. (%)
1	25	5.4	26.0	27.4	40.9	19.8	29.4
2	25	4.6	26.7	28.0	41.7	33.6	42.0
3	25	5.4	-	29.3	42.3	20.6	29.0
4	25	4.6	20.8	21.5	37.5	29.7	38.6
5	25	6.4	-	28.7	43.0	22.7	32.4
6	25	3.4	23.5	24.8	36.8	40.3	54.4
7	25	4.4	-	27.4	39.1	21.5	27.0
8	25	4.3	21.2	22.1	36.8	19.8	27.6
9	25	3.2	18.9	22.1	32.6	40.2	46.8
10	25	3.8	-	20.8	34.6	21.0	26.2
11	25	3.9	20.8	22.1	36.8	32.4	40.4
12	-196	4.0	-	90.0	93.4	6.3	13.1
13	-196	3.5	-	86.0	86.0	-	6.5
14	-196	3.0	-	90.0	95.8	1.6	10.5
15	-196	3.0	-	84.8	87.4	7.3	16.6
16	-196	2.6	-	84.0	92.6	8.1	16.9

TABLE III

(CONTINUED)

ALLOY NO. 4

Spec. No.	Test Temp (°C)	$d^{-1/2}$ ($mm^{-1/2}$)	L.Y.S. ($Kg.mm^{-2}$)	U.Y.S. ($Kg.mm^{-2}$)	Max. Tensile Stress ($Kg.mm^{-2}$)	Unif. Elong. (%)	Total Elong. (%)
1	25	6.2	-	31.3	40.4	29.0	36.0
2	25	5.8	29.0	30.3	41.0	30.8	40.6
3	25	3.0	22.8	23.5	35.2	39.5	48.2
4	25	3.3	23.5	24.8	36.5	38.6	44.0
5	25	6.3	-	30.0	41.0	23.4	32.4
6	25	6.3	-	26.7	41.0	36.2	45.2
7	27	1.8	21.5	22.1	25.4	18.4	24.4
8	25	1.6	19.6	20.5	22.8	17.0	20.5
9	25	7.0	28.7	30.0	45.0	40.0	46.0
10	25	7.1	-	26.7	44.2	38.5	43.0
11	25	3.2	20.8	22.8	36.8	34.2	41.0
12	-196	4.1	-	89.2	89.2	-	7.0
13	-196	3.3	-	86.0	86.0	-	7.2
14	-196	3.6	-	-	77.5	-	6.2
15	-196	3.7	-	-	81.5	-	29.6
16	-196	5.2	-	-	86.7	-	8.3

TALBE III

(CONTINUED)

ALLOY NO. 4

Spec. No.	Test Temp. (°C)	$d^{-1/2}$ ($mm^{-1/2}$)	L.Y.S. ($Kg.mm^{-2}$)	U.Y.S. ($Kg.mm^{-2}$)	Max. Tensile Stress ($Kg.mm^{-2}$)	Unif. Elong. (%)	Total Elong. (%)
17	-196	1.6	-	-	78.2	-	11.5
18	-196	5.6	-	94.0	94.0	-	7.7
19	-196	6.0	-	95.2	95.2	-	17.8
20	-196	5.1	-	-	88.2	-	7.3
21	-196	6.3	-	97.2	97.2	-	8.5
22	-196	3.9	-	-	82.8	-	26.0

TABLE IV

ANALYSES OF Ta-H AND Ta-Mo ALLOYS

CHARGE NO.	IMPURITY CONTENT (ppm)				
	H_2	O_2	C	N	Total
1	394	26	69	.1	490
3	33	33	39	-	105
4	62	45	34	5	146
5	60	55	31	23	169
6	66	60	21	3	90
7	130	39	28	15	222
Beam Refined Ta*	<1	35	25	10	70

ANALYSES OF Ta-Mo ALLOYS

ALLOY NO.	Mo CONTENT (at.%)
1	0.47
2	0.69
3	0.87
4	1.60

*This tantalum was electron beam refined under conditions described in reference 17.

TABLE V

MAXIMUM TENSILE STRESS VERSUS INTERSTITIAL CONTENT

FOR Ta-H ALLOYS

Alloy No.	H_2 Content (ppm)	Total Interstitial Content (ppm)	M.T.S. $d^{-1/2}=0$ ($Kg.mm^{-2}$)	M.T.S. $d^{-1/2}=4$ ($Kg.mm^{-2}$)
1	394	490	23.6	28.6
3	33	105	14.0	24.8
4	62	146	20.0	29.5
5	60	169	20.2	27.5
6	6	90	18.4	26.2
7	130	222	20.7	26.2
Pure Ta	<1	70	16.7	21.6

TABLE VI

VALUES OF σ_i AND k_y FOR

Ta-H ALLOYS AT 25°C AND $\dot{\epsilon} = 10^{-3} sec^{-1}$

Alloy No.	H_2 Content (ppm)	Total Interstitial Content (ppm)	σ_i ($Kg.mm^{-2}$)	k_y ($dyne.\ cm^{-3/2}$)
Pure Ta	<1	70	8.1	0.7×10^7
1	394	490	5.1	4.0×10^7
3	33	105	5.2	2.9×10^7
4	62	146	9.4	0.9×10^7
5	60	169	9.4	0.5×10^7
6	6	90	9.7	2.1×10^7
7	130	222	7.6	2.6×10^7

TABLE VII

VALUES OF σ_i AND k_y

FOR Ta-Mo ALLOYS

AT T = 25°C AND $\dot{\epsilon} = 10^{-3} sec^{-1}$

at.% Mo	σ_i ($Kg.mm^{-2}$)	k_y ($dyne.cm^{-3/2}$)
Pure Ta	8.5	0.7×10^7
0.87	8.5	2.0×10^7
1.60	8.5	2.9×10^7

Aeronautical Systems Division, AF Materials Lab, Metals & Ceramics Div., Wright-Patterson AFB, Ohio.
Rpt Nr ASD-TR-61-203, Part III. THE MECHANICAL PROPERTIES OF TANTALUM WITH SPECIAL REFERENCE TO THE DUCTILE-BRITTLE TRANSITION. Final report, May 63. 57p incl illus., tables, 24 refs.

Unclassified report

The tensile behavior of dilute Ta-H and Ta-Mo alloys was studied as a function of alloying addition, grain size and test temperature at a constant strain rate of 10^{-3} sec-1. The results are interpreted in terms of the parameters σ_i and k_y of the Petch equation. For Ta-H alloys at 25°C σ_i was independent of hydrogen content whereas k_y increased with hydrogen content. Deformation twinning was not observed in Ta-H alloys either at 25°C or at -196°C. Dilute additions of Mo to Ta at 25°C resulted in an increase in k_y whereas σ_i was unaffected. Twinning was observed at -196°C but not at 25°C. A large increase in ductility accompanied twinning.

(over)

1. Tantalum alloys
2. Mechanical properties
I. AFSC Project 7351, Task 735106
II. Contract AF 33 (616)-7173
III. Materials Research Corp., Orangeburg, New York
IV. G. Abowitz, R. A. Burn
V. Aval fr OTS
VI. In ASTIA collection

Aeronautical Systems Division, AF Materials Lab, Metals & Ceramics Div., Wright-Patterson AFB, Ohio.
Rpt Nr ASD-TR-61-203, Part III. THE MECHANICAL PROPERTIES OF TANTALUM WITH SPECIAL REFERENCE TO THE DUCTILE-BRITTLE TRANSITION. Final report, May 63. 57p incl illus., tables, 24 refs.

Unclassified report

The tensile behavior of dilute Ta-H and Ta-Mo alloys was studied as a function of alloying addition, grain size and test temperature at a constant strain rate of 10^{-3} sec-1. The results are interpreted in terms of the parameters σ_i and k_y of the Petch equation. For Ta-H alloys at 25°C σ_i was independent of hydrogen content whereas k_y increased with hydrogen content. Deformation twinning was not observed in Ta-H alloys either at 25°C or at -196°C. Dilute additions of Mo to Ta at 25°C resulted in an increase in k_y whereas σ_i was unaffected. Twinning was observed at -196°C but not at 25°C. A large increase in ductility accompanied twinning.

(over)

1. Tantalum alloys
2. Mechanical properties
I. AFSC Project 7351, Task 735106
II. Contract AF 33 (616)-7173
III. Materials Research Corp., Orangeburg, New York
IV. G. Abowitz, R. A. Burn
V. Aval fr OTS
VI. In ASTIA collection

Aeronautical Systems Division, AF Materials Lab, Metals & Ceramics Div., Wright-Patterson AFB, Ohio.
Rpt Nr ASD-TR-61-203, Part III. THE MECHANICAL PROPERTIES OF TANTALUM WITH SPECIAL REFERENCE TO THE DUCTILE-BRITTLE TRANSITION. Final report, May 63, 57p incl illus., tables, 24 refs.

Unclassified report

The tensile behavior of dilute Ta-H and Ta-Mo alloys was studied as a function of alloying addition, grain size and test temperature at a constant strain rate of 10^{-3} sec-1. The results are interpreted in terms of the parameters σ_i and k_y of the Petch equation. For Ta-H alloys at 25°C σ_i was independent of hydrogen content whereas k_y increased with hydrogen content. Deformation twinning was not observed in Ta-H alloys either at 25°C or at -196°C. Dilute additions of Mo to Ta at 25°C resulted in an increase in k_y whereas σ_i was unaffected. Twinning was observed at -196°C but not at 25°C. A large increase in ductility accompanied twinning.

(over)

1. Tantalum alloys
2. Mechanical properties

I. AFSC Project 7351, Task 735106
II. Contract AF 33 (616)-7173
III. Materials Research Corp., Orangeburg, New York
IV. G. Abowitz, R. A. Burn
V. Aval fr OTS
VI. In ASTIA collection

Aeronautical Systems Division, AF Materials Lab, Metals & Ceramics Div., Wright-Patterson AFB, Ohio.
Rpt Nr ASD-TR-61-203, Part III. THE MECHANICAL PROPERTIES OF TANTALUM WITH SPECIAL REFERENCE TO THE DUCTILE-BRITTLE TRANSITION. Final report, May 63, 57p incl illus., tables, 24 refs.

Unclassified report

The tensile behavior of dilute Ta-H and Ta-Mo alloys was studied as a function of alloying addition, grain size and test temperature at a constant strain rate of 10^{-3} sec-1. The results are interpreted in terms of the parameters σ_i and k_y of the Petch equation. For Ta-H alloys at 25°C σ_i was independent of hydrogen content whereas k_y increased with hydrogen content. Deformation twinning was not observed in Ta-H alloys either at 25°C or at -196°C. Dilute additions of Mo to Ta at 25°C resulted in an increase in k_y whereas σ_i was unaffected. Twinning was observed at -196°C but not at 25°C. A large increase in ductility accompanied twinning.

(over)

1. Tantalum alloys
2. Mechanical properties

I. AFSC Project 7351, Task 735106
II. Contract AF 33 (616)-7173
III. Materials Research Corp., Orangeburg, New York
IV. G. Abowitz, R. A. Burn
V. Aval fr OTS
VI. In ASTIA collection